

WEC Development Project

Winter Semester 2024/2025

Final Design Report



***OPTIMUS
SHAKTI 5.0***

Project Name: Optimus Shakti 5.0

Sub-Project: Rotor Hub and Pitch System

Prepared by:

Rahul Patil	750532
Mostafa Mozafary	750247
Eslam Mohamed	750485

Matriculation number:

Supervisor:

Mr. Christian Bulligk

Date: 24.01.2025

Acknowledgments

We would like to express our deepest gratitude to our supervisor, Mr. Christian Bulligk, for his support, guidance, and insightful knowledge throughout the entire duration of the project OPTIMUS SHAKTI. His instructions were instrumental in helping us achieve our goals.

We also extend our heartfelt thanks to Prof. Peter Quell, Prof. Torsten Faber, Mr. Andreas Manjock, Prof. Rajesh Saiju, Prof. Steffen Risius, and Prof. David Schlipf, Dr. Laurence for organizing and enabling this project. Their efforts in arranging such a collaborative initiative, including partnerships with Basaveshwar Engineering College (BEC) in India, provided us with the opportunity to work in diverse teams under their expert supervision. Their expertise and insights were invaluable assets that significantly contributed to the success of the project.

Finally, participating in this project as a representative of the Rotor Hub and Pitch System team was a remarkable experience. It felt like working on a real-world project, offering us invaluable learning opportunities and memories that we will cherish forever.

Table of contents

Acknowledgments.....	II
Table of contents.....	III
List of abbreviations	V
List of symbols.....	VII
List of Figures	XI
List of Tables.....	XIII
1. Introduction	1
2. Relevant standards and guidelines	2
2.1 Pitch System	2
2.2 Electric motor.....	3
2.3 Blade bearing.....	3
2.4 Lubrication.....	3
2.5 Bolted Connection.....	4
2.6 Hub and Spinner.....	4
3. Loads.....	5
4. Concepts Design and Calculation	7
4.1 Rotor Hub	7
4.1.1 Shapes of the Hub.....	8
4.1.2 Material of the Hub.....	9
4.1.3 CAD Design and Dimensions	10
4.2 Pitch System	11
4.2.1 Classification of Pitch system of Wind turbine	12
4.2.2 Comparison between Different concepts of Pitch System	12
4.2.3 Electric Pitch system	15
4.3 Blade bearing.....	28
4.3.1 Types of Bearings	28
4.3.2 Blade attachment.....	31
4.3.3 Dimensioning of the Three row roller bearing	33
4.3.4 Pitch bearing safety factors calculation	36

4.3.5 CAD model of Bearing and dimensions	42
4.4 Bolted Connection between Hub and Shaft.....	42
4.5 Bolted connection between Bearing and Hub	46
4.6 Lubrication System	48
4.6.1 Manual vs. Automatic Lubrication	48
4.6.2 Type of automatic lubrication systems	49
4.6.3 Grease Volume Calculation and Grease Type Selection	49
4.6.4 Typical Grease Types for Pitch Bearings.....	50
4.6.5 Lubrication Pump and Reservoir Calculation	50
4.6.6 Lubrication Pinions.....	52
4.7 Spinner	53
4.8 Complete Assembly for Rotor hub and pitch sytsem.....	54
5. Maintenance stragies	55
6. Weight and cost	57
7. Specifications of Components	58
8. Environmental Life-Cycle Assessment	61
9. Teamwork	63
10. Lesson Learned	65
11. Conclusion and Outlook.....	66
References.....	68
Annextures	72

List of abbreviations

MW	Mega Watt
GW	Giga Watt
WEC	Wind Energy Converter
CO₂	Carbon Dioxide
IEC	International Electrotechnical Commission
LCOE	Levelized Cost of Energy
DNV	Det Norske Veritas
ISO	International Organization for Standardization
MPa	Mega Pascal
OEMs	Original Equipment Manufacturers
AC	Alternating Current
DC	Direct Current
IM	Induction Motors
PMSM	Permanent Magnet Synchronous Motors
SynRM	Synchronous AC reluctance motor
TW	Terra Watt
EDLCs	Electric Double-Layer Capacitors
PF	Power Factor
U	Voltage
FC	Frequency Converter
IP	Ingress Protection
DLCs	Design Load Cases
BCD	Bolt Circle Diameter
kN	Kilo Newton
N	Newton
M	Meter

Mm	Milimeter
Kg	Kilo gram
kNm	Kilo Newton Meter
KWh	Kilo Watt Hour
L	Liter
NLGI	National Lubricating Grease Institute
LCA	Life Cycle Assessment
CAD	Computer Aided Drawings
SKF	Svenska Kullagerfabriken
WTG	Wind Turbine Generators
PF	Power Factor

List of symbols

F_{xy}	kN	Axial force
F_z	kN/m	Radial force
M_{xy}	kN/m	Bending moment
M_z	kN/m	Pitching torque
M	kN/m	Blade side moment
M_{fric}	kN/m	Friction torque of the pitch bearing
J	kg/m^2	blade inertia
φ	rad/sec^2	pitch angular acceleration
f_s	-	Bolt connection factor
W_R	kN/m	Specific friction force
D_L	m	Raceway diameter
k	-	K-factor
f_A	-	Adjacent construction factor
f_L	-	Raceway factor
μ	-	Friction coefficient
m_n	-	Gear module
D_{f2min}	m	Gear Pitch diameter
Z_{ring}	m	Number of teeth for the ring
Z_{pinion}	-	Number of teeth for the Pinion
$i_{bearing}$	-	Transmission ratio
$i_{gearbox}$	-	Gearbox ratio
M_m	kN/m	Motor torque
$M_{nominal}$	kN/m	Nominal torque
T_{OL}	kN	Overload
$M_{max,gearbox}$	kN/m	Maximum torque for pitch gearbox
$M_{max,bearing}$	kN/m	Maximum torque at bearing's teeth
M_B	kN/m	Brake torque

U_N	V	Nominal motor voltage
I_{max}	A	Maximum motor current
t	s	Time based on pitch rate
D_{pw}	mm	Bearing raceway diameter
D_w	mm	Bearing roller diameter
L	mm	Roller diameter
Z	mm	Number of Rollers
Q_{max_rigid}	kN	Maximum roller force for ideal conditions
$Q_{max_flexible}$	kN	Flexible roller force for ideal conditions
p_{max}	kN	Max Hertzian pressure
p_{0max}	kN	Ideal Hertzian pressure
$F_{t,12}$	kN	Tangential force on gear
$F_{bn,12}$	kN	Normal force on gear
$F_{rn,12}$	kN	Radial force on gear
α	Degrees	Pressure angle
$F_{t,12_nomi}$	kN	Nominal force on gear
K_a	-	The application factor
K_v	-	Dynamic factor
K_1	-	Gear quality
$K_{H\beta}$	-	Face width factor tooth width on the flank stress
$K_{F\beta}$	-	Face width factor tooth root stress
F_{sh}	μm	Elastic deformations factor
F_{ma}	μm	Manufacturing deviations factor
$F_{\beta x}$	μm	Effective flank line deviation before running-in
$F_{\beta y}$	μm	Effective flank line deviation after running-in
N_f	-	Width factor for the tooth root
$K_{H\alpha}$	-	Face load factor
K_{Fges}		Tooth base strength factor

K_{Hges}	-	Tooth flank/pitting factor
σ_{f01}	N/mm ²	The maximum local tooth root stress
Y_{fa}	-	Form factor
Y_{sa}	-	Stress correction factor
Y_{ε}	-	Overlap Factor
σ_{f12}	N/mm ²	Total tooth root stress
σ_{fg1}	N/mm ²	Tooth root limit strength
Y_{NT}	-	Service life factor
Y_X	-	Size Factor
S_{f1}	-	Safety of the tooth root load capacity
σ_{Ho}	N/mm ²	Flank pressure that occurs at the rolling point
Z_H	-	Zone factor
Z_E	-	Elasticity factor
Z_{ε}	-	Coverage factor
Z_{θ}	-	Screw factor
σ_{HG}	N/mm ²	Flank limit strength
σ_{Hlim}	N/mm ²	Tooth flank fatigue strength
Z_{NT}	-	Service life factor
Z_L	-	Lubricant factor
Z_V	-	Velocity factor
Z_R	-	Roughness factor
Z_W	-	Material pairing factor
Z_X	-	Size factor
S_{H12}	-	Safety of the flank load capacity
$F_{q_f_ges}$	kN	Axial force at shaft and hub joint
$F_{a_f_ges}$	kN	Lateral force at shaft and hub joint
$N_{S_{in}}$	-	No. of bolts (inner BCD)
$N_{S_{out}}$	-	No. of bolts (inner BCD)

$F_{q_mt_max}$	kN	Shear Force on screw by torsional moment
F_{q_F}	kN	Shear force on Bolt by External Lateral Force
r_{tmax}	mm	Outmost screw circle diameter
F_{q_ges}	kN	Total Shear force on bolt
$F_{a_mb_max}$	kN	Axial force on bolt by Bending moment
n_{SB}	-	Total number of Screws
F_{a_zd}	kN	Axial force on bolt by tensile force
F_{clamp}	kN	Clamping force on bolt
R_{p02}	N/mm ²	Proof stress of the screw material
D_{out_bcd}	mm	Bolt circle diameter of the outer race of pitch bearing
F_b	kN	Axial force carried by the bolts
f_z	-	Axial load related factor
l_k	mm	Length of clamped part
E	N/mm ²	Young's modulus for steel

List of Figures

Figure:-3. 1: Balde root Co-ordinate system [3]	5
Figure:- 4. 1: Welded Steel hub,2012, Source [5]	7
Figure:- 4. 2: Castel steel hub [5]	8
Figure:- 4. 3: Shapes of Hub ,2012. Source [6].....	8
Figure:- 4. 4: Hub CAD model of Optimus Shakti.....	10
Figure:- 4. 5: Hub CAD model of Optimus Shakti.....	11
Figure:- 4. 6: Hydraulic Pitch system ,2025 [9].....	12
Figure:- 4. 7 Electrical Pitch System,2024.Source [10].....	13
Figure:- 4. 8 Global market share of pitch concepts,2024.Source [9]	14
Figure:- 4. 9: Typical torque-speed curve of asynchronous induction motors. Source [13]....	15
Figure:- 4. 10: Typical torque and power-speed characteristic curve of PMSM AC	16
Figure:- 4. 11: Classical torque-speed characteristics of SynRM. Source [18]	17
Figure:- 4. 12: ABB Synchronous reluctance motors. Source [22]	21
Figure:- 4. 13: SEW-EURODRIVE brake components. Source [23]	22
Figure:- 4. 14: SEW-EURODRIVE brake components. Source [23]	23
Figure:- 4. 15: Delat Battery, [26]	26
Figure:- 4. 16: Sunny Tri-Power Inverter, Source [28]	27
Figure:- 4. 17: Sunny Tri-Power Inverter, Source [28]	27
Figure:- 4. 18: Double row four-point contact ball bearing external toothing,2024	28
Figure:- 4. 19: Double row four-point contact ball bearing internal toothing,2024	29
Figure:- 4. 20: Three raw rollers bearing with internal toothing ,2024. Source [30]	29
Figure:- 4. 21: Three raw rollers bearing with External toothing,2024. Source [30]	30
Figure:- 4. 22: Three raw ball and roller bearing,2024. Source [32]	30
Figure:- 4. 23: Double row angular contact ball bearing,2024.Source [33].....	31
Figure:- 4. 24: Outer Ring mounted blade,2024.Source [34].....	32
Figure:- 4. 25: Inner Ring mounted blade,2024.Source [10]	33
Figure:- 4. 26: Three rows roller bearing,2024.Source. [4]	34
Figure:- 4. 27: Forces on Gear ,2005.Source [35]	37
Figure:- 4. 28: CAD modle of Three row roller bearing of Optimus shakti	42
Figure:- 4. 29:- Loads on bolts on Rotor flange connection,2024.Source [9]	43
Figure:- 4. 30: 2 Rotor flange connection,2024.Source [9]	43
Figure:- 4. 31: Distance of bolts to bending axis,2024.Source [9]	44
Figure:- 4. 32 Lubrication Pump.....	51
Figure:- 4. 33: Lubrication Pump.....	51
Figure:- 4. 34: SKF Technical data,2024 [40]	52
Figure:- 4. 35: Lubrication and pitch pinion assembly, 2024, Source [41]	52
Figure:- 4. 36: Lubrication Pinion, Source [40].....	52
Figure:- 4. 37: Spinner Optimus Shakti	53

Figure:- 4. 38: Spinner Optimus Shakti	53
Figure:- 4. 39 : CAD model of Complete assembly of Rotor hub and pitch system	54
Figure: 7. 1 Bonfiglioli 711 TW gearbox dimensions [43]	58
Figure: 7. 2: ABB SynRM, frame size 200, dimensions [22]	59
Figure: 7. 3: SEW-EURODRIVE, magnetic brake BE30 Dimensions [23]	59
Figure: 7. 4: Lubrication pinion assembly of Oprimus shakti.....	60
Figure: 7. 5: Lubrication pinion assembly of Oprimus shakti.....	60

List of Tables

Table:-3. 1: Maximum loads extracted from simulated load sheet Appendix-A	5
Table:-3. 2: Final resulted values from simulated load sheet Appendix-A.....	6
Table:-3. 3: Loads given by Supervisor [4]	6
Table:-3. 4: Loads at hub and shaft joint [4]	6
Table:-4. 1: comparision between Spherical and Star shape hub 2012, [6]	9
Table:-4. 2: Mechanical Properties of Spheroidal cast Iron (EN-GJS-400-18) ,2014	10
Table:-4. 3: Specification of rotor hub	10
Table:-4. 4 Market share of pitch concepts in indian Market ,2024.Source [11].....	14
Table:-4. 5: Specification of Battery, Source [27]	26
Table:-4. 6:- Specification of Pitch Bearing of Optimus Shakti.....	42
Table:-4. 7: 1 Loads for Bolted joint varification, Section:-3	43
Table:-4. 8: initial data considered for the Bolted joint verification	44
Table:-4. 9:- Manual Vs. Automatic Lubrication, 2025. Source:- [38]	48
Table:-4. 10: Type of Lubrication system, 2025. Source:- [38]	49
Table: 5. 1: Maintennace startagies for Pitch bearing, Source [42]	55
Table: 5. 2: Maintennace startagies for Pitch system [42]	55
Table: 5. 3: Maintennace startagies for hub and spinner [42].....	56
Table: 6. 1:Weight of the components.....	57
Table: 6. 2: Cost of the components	57
Table: 7. 1: Specification of Pitch system components	58
Table: 7. 2: Specification of Pitch system components	59
Table: 7. 3: Specification of Pitch system components	60
Table: 8. 1 :-Co2 Emision from the Components lifecycle	62
Table: 9. 1: Work Distribution in Team	64

1. Introduction

India ranks fourth globally in wind energy, with an installed capacity of 45 GW, supported by a strong manufacturing base of 15,000 MW annually and a thriving ecosystem. The government fosters growth through incentives like Accelerated Depreciation and concessional customs duty exemptions. With 695 GW of untapped potential, India aims to achieve 140 GW by 2030, having added 2.8 GW in 2023, highlighting its dedication to renewable energy and sustainability. [1]

In line with these national goals, the OPTIMUS SHAKTI project aims to design a 5 MW onshore wind turbine tailored to the environmental conditions of the Gadag district in northern Karnataka, India. The project focuses on developing a state-of-the-art Wind Energy Converter (WEC) optimized for high energy yields in low wind speed regimes. It incorporates an integrated energy storage system to enhance capacity factors while striving for a low economic footprint, reduced CO₂ emissions, and high recyclability. The design targets a power density of 200 W/m² within a market-safe supply chain and adheres to Wind Type Class IEC III(b), suitable for mean wind speeds of 7.5 m/s. The ultimate objective is to achieve the Levelised Cost of Energy (LCOE) while maintaining efficiency and environmental responsibility.

To accomplish this, the project is divided into 10 specialized sub-teams: Project Management, Loads and Dynamics, Dynamic Control, Control Strategy, Rotor Blades, Electrical Drivetrain, Rotor Hub & Pitch System, Rotor Bearing System, Gearbox Coupling Brake, Machine Bed & Yaw System, Energy Storage, and Tower and Foundation. Each team is tasked with designing and developing their respective components to ensure the successful integration and functionality of the wind turbine system.

As part of this effort, our team is responsible for designing the rotor hub and pitch system, including critical components such as the pitch bearing, pitch motor, pinion, lubrication system, and spinner. Furthermore, this team works closely with the Rotor Blades and Main Bearing teams to ensure seamless integration and coordination, a key factor for the project's overall success.

Mostafa Mozafary, Islam Mohammed and Rahul Patil are the members of rotor hub and pitch system team, which was guided by Mr. Christian Bulligk.

2. Relevant standards and guidelines

The design of wind turbines must achieve certain objectives such as ensuring regular operational conditions, safeguarding personnel and equipment, and minimizing risks to human life. The structures and components should meet their expected lifespan, and the overall system must demonstrate a sufficient level of reliability.

To meet these goals, wind turbines must be designed according to standards that provide principles, technical requirements, and guidelines for the design and manufacturing of machinery components and structures for wind turbines. These standards ensure safety and performance in both ultimate and serviceability limit states.

For our project the Optimus Shakti, we are following DNV standards. ‘Machinery for wind turbines – DNV-ST-0361’ was consulted to establish standards for designing the Rotor hub and Pitch system components. The design requirements for components are outlined below. [2].

2.1 Pitch System

For pitch systems with a pitch gearbox, the strength analysis of the pitch system shall include the pitch gearbox teeth, the blade bearing teeth, the load capacity considering the fatigue loads, static strength against tooth breakage and pitting (Sec.7.2.2.1- [2]).

For the calculation of the loading of the blade pitching system, the design loads as per section 4 of DNV-ST-0437 shall be applied.

In case of pitch systems with a pitch gearbox, the gear load capacity calculation of the pitch gearbox and pitch teeth shall be based on the ISO 6336 series. Additionally, a static strength analysis should be conducted to evaluate the resistance to tooth breakage and pitting, ensuring adherence to the specified safety factors. The safety factors for pitting are defined as 1.0 for the gearbox teeth and 1.0 for the pitch system teeth. For tooth root breakage, the safety factors are specified as 1.1 for the gearbox teeth and 1.2 for the pitch system teeth. (Sec.7.4.2.1- [2])

For the bearings in the actuators of pitch and yaw systems, the static safety factor S_0 according to ISO 76:2006 shall be at least 1.1. (Sec.6.5.1.4- [2])

The locking devices shall be so designed that even with a brake removed they can reliably prevent any rotation of the rotor, nacelle or the rotor blade. The locked (engaged) and the unlocked (disengaged) position of the locking devices shall be secured against unintentional locking and unlocking as per Sec.-7.5- [2].

2.2 Electric motor

Motors shall be designed according to the operating times and temperatures to be expected. The designed duty types shall be given as specified in IEC-60034 Part-1 ‘Rating and Performance’. (Sec.7.2.4.5- [2])

The nominal torque (M_n) and the equivalent torque (reference torque) of auxiliary motors (e.g. pitch motor) shall be in compliance with the corresponding load calculations [2].

2.3 Blade bearing

For blade and yaw bearings, which experience primarily small back-and-forth motions, the static rating is directly calculated from the maximum contact stress between rolling elements and the raceway. The maximum allowable Hertzian contact stress must be specified by the bearing manufacturer, considering factors such as material, surface hardness, and hardening depth. This value should be documented in the design calculations.

The static safety factor for blade and yaw bearings is the ratio between the maximum permissible Hertzian contact stress and the maximum contact stress, and it should be at least 1.1 according to Sec.-6.5.1.3. [2].

The maximum permissible Hertzian contact stress of 4000 MPa for all the roller bearings defined by the ISO 76:2006.

2.4 Lubrication

A consistent supply of lubricant must be maintained on the blade bearing teeth and between rolling elements and the track surface for all wind turbine operations.

A lubrication system is required for the teeth, and its functionality must be documented. If needed, this can be verified through a test run, typically performed once every 24 hours. During this test, the rotor blades and blade bearings should be rotated to ensure adequate relubrication.

Proper collection reservoirs should be provided to handle excess lubricant from the blade bearing components. (Sec.-7.4.2.12- [2])

2.5 Bolted Connection

Analytical calculations of axially loaded bolted joints should be performed on the basis of VDI 2230 or other widely recognized design codes and analytical methodologies [2].

2.6 Hub and Spinner

For the Hub, cast iron with spheroidal graphite (EN-GJS) according to EN 1563:2012-03 may be used, depending on the mechanical properties required.

Without additional verification, cast iron with a fracture elongation $A < 12.5\%$ or an impact energy $K_{vmean} < 10 \text{ J}$ (mean value of three tests) shall not be used for components that play a significant role in the transmission of force and are under high dynamic loading, e.g. rotor hub.

For requirements for manufacturers such as used material, bonding process, building-up the laminates, curing time, resin application and finishing process of nacelle covers and spinners made of fiber-reinforced plastics (FRP), refer to Sec.5 of DNV-ST-0376.

Areas of spinner that exhibit the hazard of falling from height or slip-trip shall be equipped with suitable safety attachment points as per Sec.11.2.5- [2].

3. Loads

The simulated loads for the Optimus Shakti, provided by the load team (refer to Annexure-A), detail the maximum forces and moments acting on the blade root. The peak values from these simulations have been extracted and are presented in the following table.

F_x (kN)	F_y (kN)	F_z (kN)	M_x (kNm)	M_y (kNm)	M_z (kNm)
1034.29	779.43	2737.20	23056.8	49553.14	619.601413

Table:-3. 1: Maximum loads extracted from simulated load sheet Annexure-A

The values presented represent the extreme loads obtained from various simulations, acting along the blade root coordinate system, as illustrated in the subsequent image.

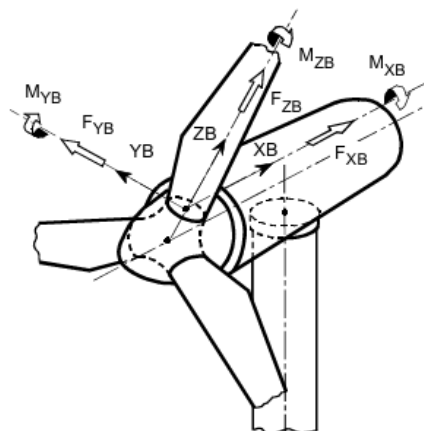


Figure:-3. 1: Balde root Co-ordinate system [3]

The first three forces in the table above are the principal forces in x, y, z direction. M_x is the edge wise bending moment around the x-axis as pictured above whereas, M_y is the flap-wise moment around the y-axis. Lastly there is the pitching torque M_z around the z-axis.

The first three forces F_x , F_y and F_z listed in the table above, represent the principal forces along the x, y, and z directions, respectively. M_x denotes the edgewise bending moment about the x-axis, as depicted above, while M_y corresponds to the flap wise bending moment about the y-axis. Lastly, M_z represents the pitching torque about the z-axis.

F_x and F_y acts as a combined axial load F_{xy} , similarly, M_x and M_y acts as combined moment at the blade root M_{xy} . So, the following table gives the final resulting values of loads.

Axial Force (F_{xy})	Radial force (F_z)	Bending Moment (M_{xy})	Pitching Torque (M_z)
1908.5 kN	2737.5 kN	31260 kNm	619.6 kNm

Table:-3. 2: Final resulted values from simulated load sheet Appendix-A

However, the resulting loads are significantly high for use as the basis for calculating the pitch system components and bearings. Utilizing these loads for designing the Optimus Shakti components may lead to non-competitive designs in terms of dimensions and cost-efficiency. Furthermore, these loads were provided by the loads team at the final stage of the project, making design modifications based on the given values unfeasible. Consequently, the components such as pitch system and bearing were designed based on the loads provided by our supervisor, as outlined below.

Axial Force (F_{xy})	Radial force (F_z)	Bending Moment (M_{xy})	Pitching Torque (M_z)
900 kN	800 kN	40000 kNm	500 kNm

Table:-3. 3: Loads given by Supervisor [4]

Similarly, for the bolted joint calculations between the hub and shaft, the loads were provided by our supervisor, as detailed below. These specified loads were derived from a similar size wind turbine and were utilized for subsequent calculations.

Axial Force	Lateral Force	Bending Moment	Torsional Moment
$F_a_f_{ges}$	$F_q_f_{ges}$	M_b	M_t
700 kN	2000 kN	25000 kNm	12000 kNm

Table:-3. 4: Loads at hub and shaft joint [4]

4. Concepts Design and Calculation

4.1 Rotor Hub

The rotor hub serves as the initial component of the mechanical drive train. While it is technically part of the rotor, it is functionally and structurally closely linked to the mechanical drive train. Hub serves as the fixture for connecting the rotor blades to the main shaft and transmitting the rotational energy generated by the blades to the mechanical drive train. In pitch-controlled wind turbines, the hub houses the components of the blade pitch mechanism enabling the adjustment of blade angles to optimize energy capture and manage turbine performance under varying wind conditions. [5]

The rotor hub is among the most heavily stressed components of a wind turbine, as it bears the concentrated rotor forces and moments at a single point. Consequently, its material must be chosen with utmost care to ensure durability and fatigue resistance. This necessitates extensive and meticulous work in strength calculations and dimensioning to prevent localized stress concentrations. [5]

There are essentially three possible solutions concerning the selection of materials and the associated design and construction:

- Welded sheet steel
- Cast steel
- Forged steel.

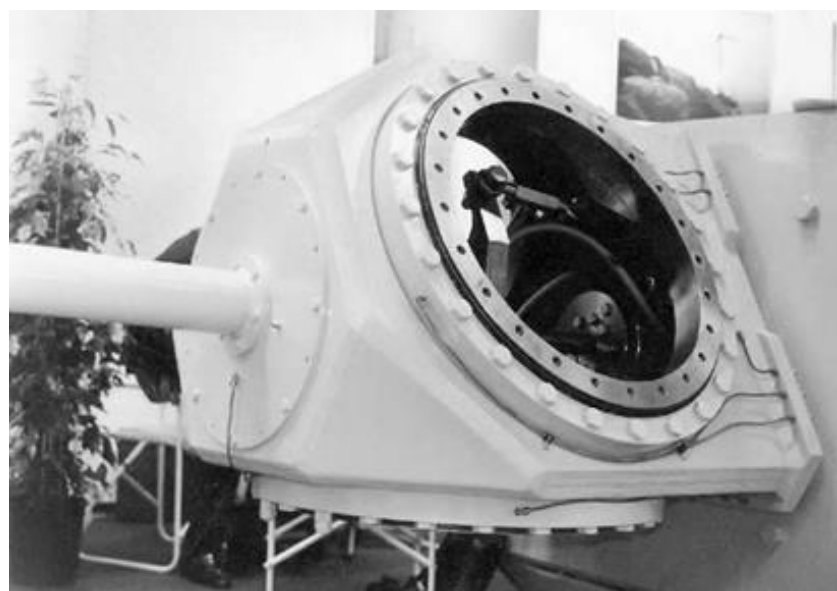


Figure:- 4. 1: Welded Steel hub,2012, Source [5]

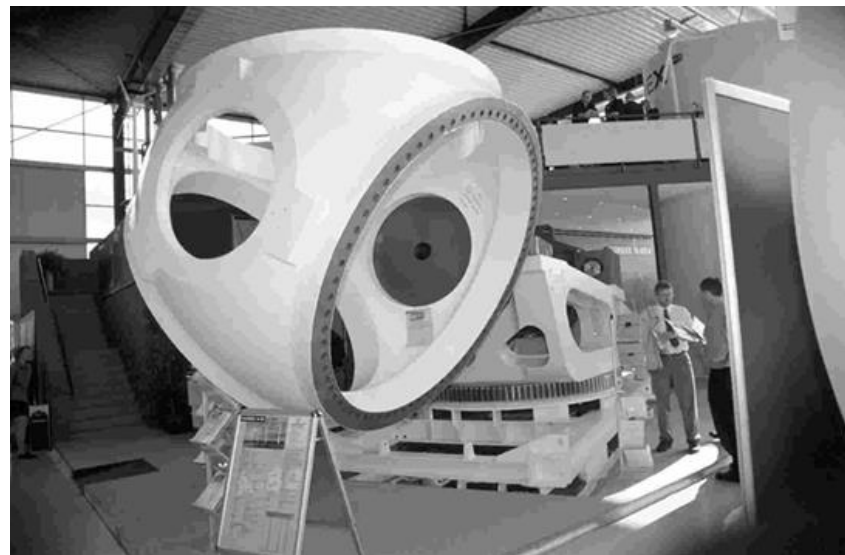


Figure:- 4. 2: Castel steel hub [5]

In the past, all three variations could be found in wind turbines. In the course of time, the cast steel hub has become generally accepted. The technology of cast materials has, however, made considerable progress since then and a much more suitable material for components having dynamic load spectrum has been found to be a spheroidal graphite cast-iron.

The cast hub can be shaped with smooth contours following the load paths. Local stress peaks, resulting from corners and from discontinuities in the wall thickness profile, are avoided.

4.1.1 Shapes of the Hub

For casted hubs in modern wind turbines, three popular designs are commonly used: the spherical shape, b) the star shape, and c) the topologically optimized hub, as illustrated in Figure 4.3 :- Shapes of Hub.

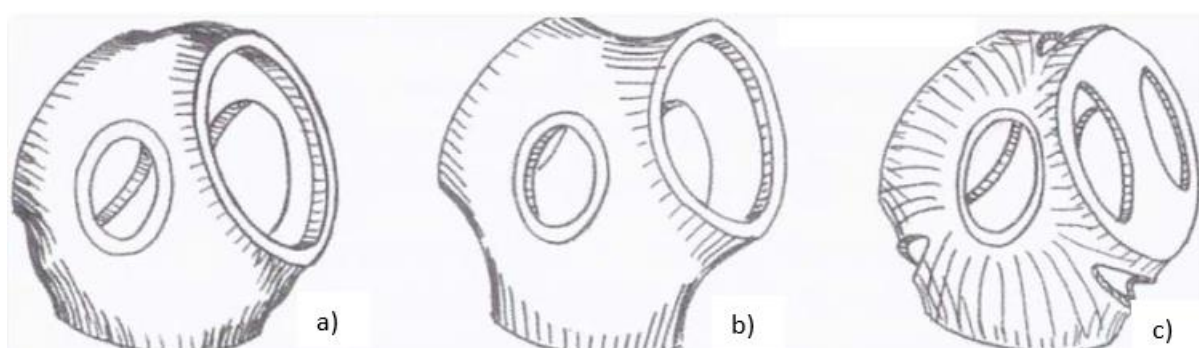


Figure:- 4. 3: Shapes of Hub ,2012. Source [6]

Comparison between spherical and star shape hub as these two shapes are the basis to start the hub design. And then, the computational approach used to minimize material usage while maintaining structural integrity and resulting design called Topologically Optimized design.

Spherical shape hub	Criteria	Star shape hub
Follow curvature	Load direction	Straight
Distributes stress more evenly due to its symmetrical geometry.	Stress concentration	Stress is concentrated along the arms and connection points, requiring careful design.
Offers lower aerodynamic drag in some cases due to smooth surfaces.	Aerodynamic Performance	May generate slightly higher drag due to sharp edges or protrusions.
Heavier and less costly	Weight and Cost	Lighter and Higher production cost due to complexity
Easier to manufacture due to its simple geometry.	Manufacturing	Requires more complex manufacturing techniques to shape the arms accurately.
High durability due to even stress distribution.	Durability	Requires precise engineering to avoid fatigue or failure at stress points.

Table:-4. 1: comparision between Spherical and Star shape hub 2012, [6]

To conclude, the spherical-shaped hub ensures uniform stress distribution, enhancing durability and reliability. Its simple design is easier and more cost-effective to manufacture, and the smooth surface minimizes aerodynamic drag. This design is ideal for robust performance in varied conditions and medium-sized wind turbines. These factors make the spherical shape the preferred choice for the Optimus Shakti wind turbine.

4.1.2 Material of the Hub

Spheroidal cast iron (EN-GJS-400-18) is a highly suitable material for wind turbine hubs, offering an exceptional combination of strength and ductility that allows it to withstand both high and cyclic loads efficiently. Its strong fatigue resistance ensures durability over extended periods, while the economical casting process facilitates the creation of intricate hub designs. Additionally, the material's excellent machinability streamlines precision manufacturing, and its moderate corrosion resistance makes it well-suited for challenging environmental conditions. These benefits, coupled with its established track record in wind turbine applications, make it a reliable and cost-effective option for hub construction. [7]

Spheroidal cast Iron (EN-GJS-400-18)		Value
Tensile strength		360 MPa
Compressive Strength		275 MPa
Yield strength		220 MPa
Young's Modulus		169 GPa
Density		7100 Kg/m ³
Poisson's ratio		0.28

Table:-4. 2: Mechanical Properties of Spheroidal cast Iron (EN-GJS-400-18) ,2014. Source [8]

4.1.3 CAD Design and Dimensions

Rotor Hub	
Hub diameter	5088 mm
Cone angle	5°
Total weight	70 T
Material	EN-GJS-400-18
Hub to shaft BCD	2340 mm (Outer)
	2140 mm (Inner)
Bolts on inner BCD	56*M39
Bolts on outer BCD	60*M39
hub length	4600 mm

Table:-4. 3: Specification of rotor hub



Figure:- 4. 4: Hub CAD model of Optimus Shakti

Hub accessibility for maintenance

Three manholes are considered on the hub, making it possible for operators to get into the hub for maintenance. Operators from inside the nacelle can easily reach the manholes with the relevant ladder, and then, using the ladders mounted inside the hub, safely reach inside the hub.

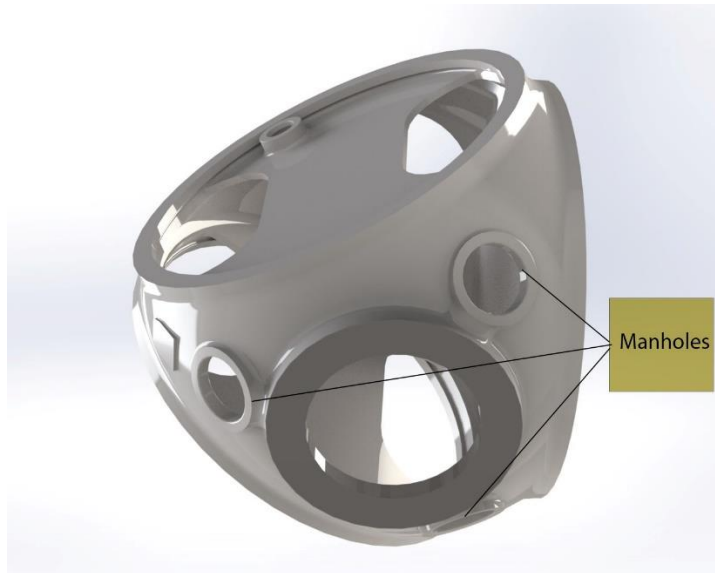
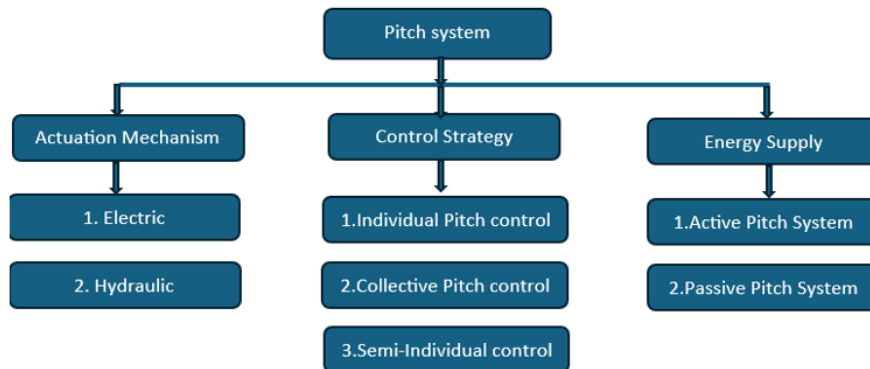


Figure:- 4. 5: Hub CAD model of Optimus Shakti

4.2 Pitch System

In existing wind turbine technology, all wind turbines are equipped with rotors that utilize blade pitch control called the ‘Pitch System’. This mechanism serves several purposes. The first is to regulate the blade pitch angle, which is essential for controlling the rotor's power output and speed. Typically, a pitching range of 20 to 25 degrees is sufficient to achieve this. This operation functions in case of power optimization, power limitation, and sound operation modes. The mechanism has a secondary function that significantly impacts its design. To enable the aerodynamic braking of the rotor, the blades must be able to pitch to a feathered position. This requirement expands the pitching range to approximately 90 degrees to stop the wind turbine as well as to protect it from the over speeding in extreme weather conditions. Additionally, it aids in reducing the load on the turbine by adjusting the angles of individual blades. [5]

4.2.1 Classification of Pitch system of Wind turbine



4.2.2 Comparison between Different concepts of Pitch System

Modern wind turbines commonly use either hydraulic or electric pitch systems, that will be discussed in the following sections.

4.2.2.1 Hydraulic Pitch System

The hydraulic pitch system functions by maintaining a continuous supply of hydraulic pressure from a power unit, with the fluid delivered through a rotary lead-through and a hollow shaft to the hub. Within the hub, the pitch controller manages valves to direct hydraulic fluid to the pistons, which adjust the rotor blade pitch by extending and retracting. For safety, hydraulic fluid is stored in pressure tanks located in the hub, allowing the blades to move to a feathered position during emergencies. In such situations, a valve releases the stored fluid, driving the piston to position the blades safely as shown in figure. [5]



Figure:- 4. 6: Hydraulic Pitch system ,2025 [9]

The hydraulic system has advantages such as delivering high power output with compact components, high reliability, fewer parts (eliminating gears), no backlash, and no need for tooth lubrication. However, it also has notable drawbacks, including the risk of fluid leakage, higher maintenance requirements, lower efficiency, and increased energy consumption since the pump operates continuously. Additionally, operational costs are elevated due to regular maintenance, including replacing cylinder seals, tubes every 5–10 years, and periodic oil and filtration replacements [9].

4.2.2.2 Electric Pitch System

Modern MW-class wind turbines use electric pitch systems with a planetary gear connected directly to the motor. The motor's torque is transmitted through the gear to drive the pinion wheel, which rotates the blade's gear ring. The planetary gear reduces the high torque required to move the blade and adjusts the motor's speed to match the low rotational speed of the pitch system. For safety, each pitch motor has its own power storage unit, like lithium-ion batteries or capacitors, to ensure operation during power outages. [5]



Figure:- 4. 7 Electrical Pitch System,2024.Source [10]

The electrical system offers significant advantages, including high efficiency with quick responses, low maintenance requirements, and quiet operation, making it ideal for environments sensitive to noise. However, its complexity, higher chance of failure, and the need for gear lubrication are some drawbacks. [9]

4.2.2.3 Market Share of Pitch system concepts

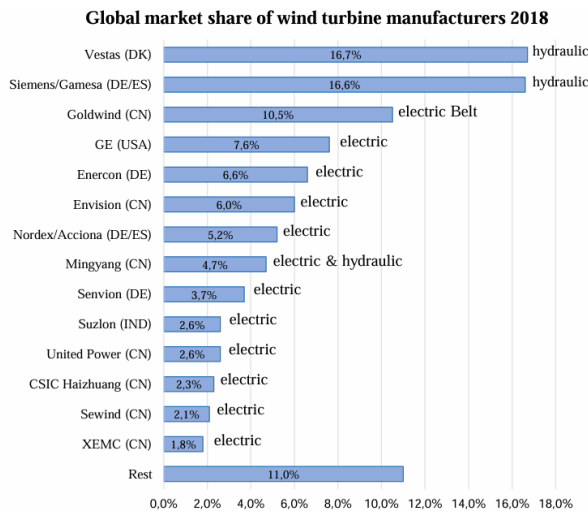


Figure:- 4. 8 Global market share of pitch concepts,2024.Source [9]

As demonstrated by the data, the electric pitch system is increasingly favored by manufacturers in comparison to the hydraulic pitch system. Approximately 60% of manufacturers opt for the electric pitch system, a trend that is similarly reflected among Wind Turbine Generators (WTGs) OEMs in India, where over 77% of manufacturers rely on the electric pitch system.

S.No	OEM	WTG Model	Pitch System
1	Adani New Industries Limited	MWL-160-5.2MW	Electrical
2	Envision Wind Power Technologies India	EN-156/3.3 MW	Electrical
3	Suzlon Energy Limited	S120 DFIG 2.1 MW (50 Hz)	Electrical
4	Vestas Wind Technology India Private Limited	Vestas V100-2MW	Hydraulic
5	Siemens Gamesa Renewable Power Private Limited	SG 2.2-122	Hydraulic
6	Sany Wind Energy India Private Limited	SI-16840 (4 MW)	Electrical
7	GE India Industrial Private Limited	GE 2.7 - 132	Electrical
8	Inox Wind Limited	INOX DF/3000/145	Electrical

Table:-4. 4 Market share of pitch concepts in Indian Market ,2024.Source [11]

Despite certain challenges, the electric pitch system's cost-effectiveness and operational efficiency make it a preferred choice for manufacturers globally. These attributes have been key factors in its selection for the Optimus Shakti

4.2.3 Electric Pitch system

The electric pitch system in a wind turbine consists of several key components that work together to adjust the blade pitch angle for optimal performance and safety. At its core is the electric pitch motor, pitch drive and back-up system.

4.2.3.1 Electric Motor

Fundamentally, two types of electric motors are available for the pitch actuator of wind turbines: AC and DC, both of which have their pros and cons. Generally, AC motors are cheaper and require less maintenance, which is why they are more common in current designs. On the other hand, DC motors are more expensive but can be directly powered by an emergency power supply without requiring an additional converter.

However, we briefly investigate all available types and, based on the project priorities, choose the one that best matches.

a) Asynchronous induction motors (IM):

The conventional three-phase AC induction motor is a constant-speed motor that can be easily used in variable-speed applications, albeit typically with reduced efficiency. [12] The squirrel cage rotor induction motor (IM) has low starting torque and a high starting current.

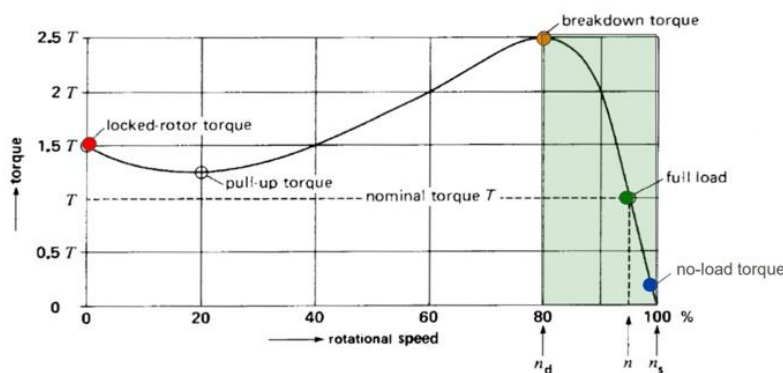


Figure:- 4. 9: Typical torque-speed curve of asynchronous induction motors. Source [13]

The torque of an IM is directly proportional to the product of the flux per pole, the rotor current, and the rotor's power factor. The maximum torque, also known as the breakdown torque, depends on the rotor reactance per phase at standstill and is independent of the rotor resistance per phase. However, the speed, or slip, at which it occurs is determined by the rotor resistance per phase. [14]

b) Permanent magnet motors (*PMSM*):

The permanent-magnet synchronous motor (*PMSM*) offers numerous advantages over other types of machines traditionally used for *AC* servo drives. It has a higher torque-to-inertia ratio and greater power density compared to an induction motor or a wound rotor synchronous motor. This makes it suitable for applications such as robotics and aerospace actuators. However, it is challenging to control due to its nonlinear dynamic behavior and time-varying parameters. [15]

Unlike induction motors, the torque-speed characteristic of a *PMSM* does not involve slip, as the rotor is synchronized with the stator's magnetic field. Instead, torque is controlled directly by regulating the I_q component of the stator current.

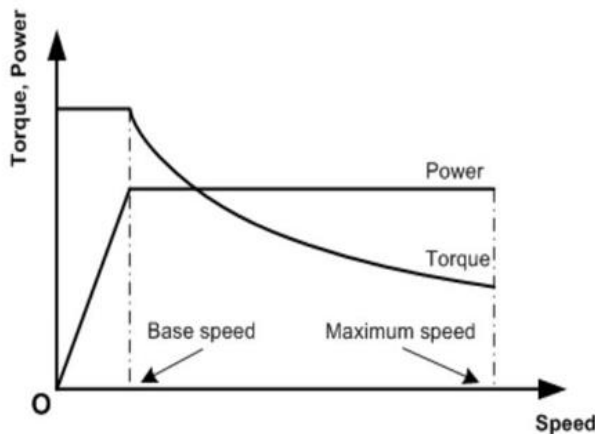


Figure:- 4. 10: Typical torque and power-speed characteristic curve of PMSM AC. Source [16]

c) Synchronous AC reluctance motor (*SynRM*):

The rotor design of a *SynRM* distinguishes it from its *IM* and *PMSM* counterparts. Compared to these conventional motors, *SynRM* achieves higher reliability and easier maintenance (due to very low winding and bearing temperatures, as well as the absence of a cage or *PMs* in the rotor structure), lower cost (due to the lack of *PMs* compared to *PMSM*), faster dynamic response (due to its smaller size within the same power range and lower moment of inertia), a higher speed range (due to wide constant-power operation compared to *IM*), and higher efficiency within the same power range and frame size (due to cold rotor operation compared to *IM*, and higher power density and torque per ampere compared to *IM*). In this sense, *SynRM* offers the high performance of *PMSM* while remaining as inexpensive, simple, and service-friendly as *IM*. [17]

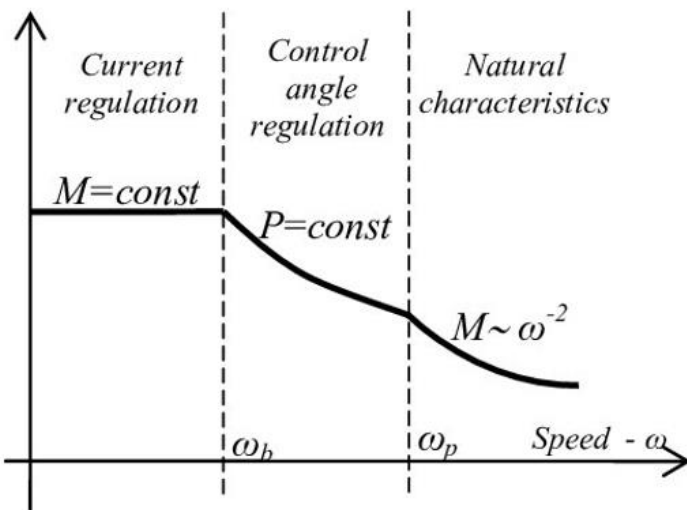


Figure:- 4. 11: Classical torque-speed characteristics of SynRM. Source [18]

d) Direct current DC motors:

The *DC* motor consists of a stator and a rotating part, the armature, separated by an air gap. The armature is wound with coils that are connected to a commutator. During rotation, the polarity of the armature winding is changed through the sliding contacts (carbon brushes) running on the commutator, thereby generating constant torque.

If *DC* motors are used in applications requiring relatively high positioning accuracy, servo technology can be integrated into the *DC* machines. The additional module required for this is an encoder system, which can take the form of a resolver, an incremental encoder, or, more commonly, an absolute encoder. This enables the exact speed of the motor to be measured and the precise position of the armature to be determined. [19]

4.2.3.2 Pitch drive selection

In this project, the design priorities are cost, reliability, and low weight. In terms of cost, asynchronous induction motors (*IM*) and synchronous AC reluctance motors (*SynRM*) are more favorable. However, as mentioned earlier, *SynRM* offers higher performance compared to *IM*. Therefore, *SynRM* has been chosen for this project.

Pitch actuator static calculation:

In the pitch actuator calculation procedure, torque and rotational speed are two important parameters that should be investigated. Additionally, regarding torque, we first calculate the required torque on the blade side. Then, we examine whether the selected pitch actuator from the market can fulfill the required torque as well as the rotational speed.

Required torque on the blade-side:

However, the required torque on the blade side consists of three parts, the acting wind torque (M_z), the friction torque of the pitch bearing (M_{fric}), and the torque obtained from blade inertia (J). The relevant equation is shown in 1.1. and $\ddot{\varphi}$ is pitch angular acceleration [20].

$$M = M_z + M_{fric} + J \cdot \ddot{\varphi} \quad (4.1)$$

The inertia of blade about the pitch axis is J [kg/m^2] and the pitch angular acceleration is $\ddot{\varphi}$ [rad/sec^2]. While the desired pitch angular speed is assumed $2 deg/sec$ to convert it to rad/sec we have:

$$2 deg/sec \times \frac{\pi}{180} = \frac{\pi}{90} rad/sec \approx 0.0349 rad/sec$$

The friction of the pitch bearing comes with highest uncertainty; it depends on the type of bearing, the number of rolling elements, and the lubrication system. Which in Optimus Shakti pitch bearing is a three-row roller bearing [20].

However, to estimate the friction torque of the pitch bearing, we have used equations provided by bearing manufacturer. The overall friction torque is made up of rolling friction, dynamic friction and lubricant friction. [21]

$$M_{fric} = M_E + M_{RN} \quad (4.2)$$

$$M_{fric} = f_s \cdot W_R \cdot D_L^2 + k \cdot \mu \cdot f_A \cdot 0.95 \cdot e^{(0.15 \times n_{GWL})} \cdot (M_{xy} + \frac{f_L \cdot F_R \cdot D_L}{2} + \frac{F_A \cdot D_L}{k}) \quad (4.3)$$

f_s : Bolt connection factor = 1.05

W_R : Specific friction force [kN/m] = 1.53

D_L : Raceway diameter [m] = 3.8

k : K-factor = 1.17

f_A : Adjacent construction factor = 1

n_{GWL} : Speed of the large diameter bearing. (*neglected*)

f_L : Raceway factor $f_L = 1.73$ (constant)

μ : Friction coefficient = 0.0015

F_A : Axial load [kN] = 800

F_R : Radial load [kN] = 900

Bending moment [kNm] = 500

* M_{xy} , F_A , F_R are obtained from section 3.

So, we have:

$$M_{fric} \cong 1.05 \times 1.53 \times 3.8^2 + 1.17 \times 0.0015 \times 1 \times 0.95 \times e^{0.15} (40000 \times 10^3 + \frac{1.73 \times 900 \times 10^3 \times 3.8}{2} + \frac{800 \times 10^3 \times 3.8}{1.17}) \cong 88.271 \text{ kNm}$$

The acting wind torque M_z varies with different pitch angles and wind speeds, so an aeroelastic simulation is required. On the other hand, the acting wind torque can either be supportive or not, depending on direction of rotation.

Based on Section 3, the total required torque to turn blade in the ring of the pitch bearing with a safety factor is:

$$M = M_z + M_{fric} + J \cdot \ddot{\phi} + 50 = 500 \text{ KNm} \quad (4.4)$$

*50 kNm added as the safe factor.

Provided torque on motor-side:

initial data:

- Bolt Circle diameter of the blade (BCD) = 3600 mm
- Gear Module (m_n) = 16 mm
- Gear Pitch diameter (D_{f2min}) = 3474 mm
- Number of teeth for the ring (Z_{ring}) = 217
- Number of teeth for the Pinion (Z_{pinion}) = 16

The transmission ratio of the bearing and the pinion:

$$i_{bearing} = Z_{ring}/Z_{pinion} \quad (4.5)$$

$$i_{bearing} = 217/16 = 13.56$$

The required torque in the pinion of the gearbox:

$$M_{pinion} = (M) / (i_{bearing} \times \eta_{ring}) \quad (4.6)$$

$$M_{pinion} = \frac{500}{13.56 \times 0.96} = 38.41 \text{ kNm}$$

Regarding the gearbox of pitch motor, while we know three stages gearbox is common therefore, we assumed 170 as its ratio:

$$i_{gearbox} = 170 \quad (4.7)$$

Total pitch system ratio is

$$i_{total} = i_{bearing} \cdot i_{gearbox} \quad (4.8)$$

$$i_{total} = 13.56 \times 170 = 2305.2 \quad (4.9)$$

Obtaining the motor torque M_m depends on the transmission ratio between the pinion and the blade bearing ring ($i_{bearing}$) and the electric motor gearbox ratio ($i_{gearbox}$). Moreover, losses in teethes, gearbox, motor and converter increase the required power as well.

$$M_m = M / (i_{total}) \quad (4.10)$$

$$M_m = 500 / 2305.2 = 0.217 \text{ kNm} = 217 \text{ Nm} \quad (4.11)$$

Since the system's efficiency is not 100%, an additional 40 kNm is incorporated to account for losses.

On one hand, 257 Nm represents the maximum torque pitch motor should provide. On the other hand, in Optimus Shakti dynamic load is not available so we do not know for how long we need this maximum torque therefore we assume it needs in short time.

Next, we investigated the available electric motors in the market to find a suitable one. We chose IE5 Synchronous AC reluctance motor from *ABB* with a frame size is 200M a nominal power 18.5 KW and a nominal rotational speed ($6P$) = $1000 \text{ } 1/\text{min}$. The nominal torque is $M_{nominal} = 177 \text{ NM}$ while the maximum rotational speed can reach $4500 \text{ } 1/\text{min}$ and the ratio between the overload and nominal torque is $T_{OL}/T_n = 1.5$. [22]

IE5 synchronous reluctance motors, network voltage 400 V												
Output, kW	Type designation	Product code	Speed at 100% of nominal power	IE class acc. to IEC	Motor efficiency with VSD supply	Typical IE3 induction motor efficiency with VSD supply*	Max speed, n_{max}	Current, I_n A	Torque	Rotor inertia ($J = 1/4GD^2$)	Weight, Kg	Tempera- ture rise class (M)
18.5	M3BL 200MLA 4 3GBL202412-B5C	1000	IE5	95.2	90.6	4500	39.9	177	1.5	0.287	304	B
1000 r/min (33.3 Hz)			400 V network									
									T_n / T_{co}			
									Nm / Nm			

Figure:- 4. 12: ABB Synchronous reluctance motors. Source [22]

Based on the selected electric motor, we examine the torque provided by the motor against the required maximum blade-side torque to determine if it is sufficient to counteract it. So:

$$M_m + \text{losses} = M_{\text{overload motor}} \quad (4.12)$$

$$257 \leq 177 \times 1.5$$

$$257 \leq 265.5$$

Regarding the selecting of the proper gearbox, the *ABB* motor with frame size 200M and mounting configuration IM B5 is fully compatible with the Bonfiglioli 711TW gearbox due to its adherence to IEC standardized flange dimensions.

Therefore, the maximum torque for pitch gearbox is equal to:

$$M_{\text{max,gearbox}} = 177 \times 1.5 \times 170 = 45.135 \text{ kNm} \quad (4.13)$$

In term of maximum torque will be implemented to blade bearing's teeth:

$$M_{\text{max,bearing}} = 177 \times 1.5 \times 13.56 = 612.03 \text{ kNm}$$

While dynamic loads were not available for the Shakti Optimus project, we assumed that the selected drive is feasible under all probable conditions.

Brake:

Electromagnetic disc brakes operate using a set of springs and are disengaged when voltage is applied to the brake coil. This ensures that the motor automatically engages the brake in the event of a voltage failure, providing an important safety feature. The brake remains effective regardless of the motor's mounting position, and the external dimensions are the same for both DC and three-phase AC brakes. [22]

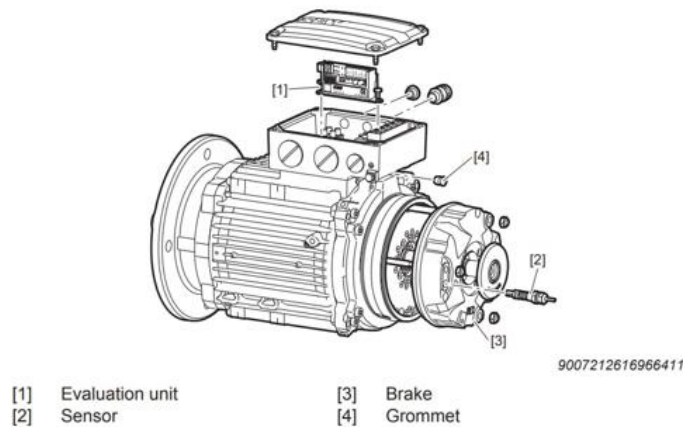


Figure:- 4. 13: SEW-EURODRIVE brake components. Source [23]

The electro-magnetic disc brake is powered, by either DC current through a rectifier located in terminal box or three phase AC current. When the brake coil is de-energized, the brake is actuated by spring pressure. The axial movement of the brake disc performs a dual braking action against the moving electromagnet and the motor shield, without pressure or impact being transmitted to the bearings.

Therefore, based on the gear ratios of the blade bearing, the gearbox, and section 3, we have:

$$M_B = \frac{\text{Brake torque}}{i_{\text{bearing}} \cdot i_{\text{gearbox}}} \quad (4.14)$$

$$M_B = \frac{500 \cdot 10^3}{13.56 \cdot 170} = 216.9 \text{ Nm}$$

M_B = Maximum required brake torque

Next, we investigated the available brakes on the market to find a suitable option. While all brakes adhere to relevant standards, it is possible to use brakes from different manufacturers. Considering the frame size of the selected motor 200M and the required brake torque, we

chose the *BE30* brake from *SEW – EURODRIVE*. The table below shows the nominal brake torque and the compatibility of the brake with different motor frame sizes.

Braking torque (M_B)	BE30	BE32	BE60	BE62	BE120	BE122
75						
100						
150						
200						
300						
400						
500						
600						
800 ¹⁾						
1000 ¹⁾						
1200 ¹⁾						
1600 ¹⁾						
2000 ¹⁾						

Figure:- 4. 14: SEW-EURODRIVE brake components. Source [23]

Torque adjustment is possible by adjusting the air gap in the brake. The nominal brake torque for the BE30 is 300 Nm, which is greater than the calculated maximum required brake torque.

Availability of Brake and Gear Motor in the Indian Market:

All selected products have been chosen with notice to availability in India market which make it easier to reach products as well as spare parts. Below we provide the current address of manufacturers of brake, electric motor and actuator's gearbox.

- Synchronous AC reluctance motor Brand: ABB Address: Disha - 3rd Floor, Plot No.5 & 6,2nd Stage,Peenya Industrial Area IV,Peenya560058 Bangalore, Karnataka, India
- Electromagnetic brake: Address: SEW-EURODRIVE INDIA PRIVATE LIMITED, Plot No.4, GIDC Por, Ramangamdi, Vadodara-391 243, Gujarat, India.
- Actuator's gearbox: Brand: Bonfiglioli Drive Systems Pvt. Ltd Address: No 50, Papparambakkam Road, Mannur Village, Sriperumbudur Taluk, Kancheepuram - 602105, Tamil Nadu

4.2.3.3 Back-up Supply system

Wind turbines are increasingly relied upon to contribute to electricity generation. However, their operation is influenced by variable wind conditions and extreme weather, ranging from very cold to very warm temperatures. A critical component of wind turbines is the pitch control system, which continuously adjusts the blades' angle to optimize performance under changing wind conditions. Additionally, it ensures the blades can be rotated to a safe position during emergencies or when wind speeds become dangerously high. This is typically achieved using a combination of generated electricity and a parallel-connected battery. The battery plays a vital role in handling the highly dynamic and variable load demands, including power peaks. It also serves as the backup power source if the main power supply is lost. Therefore, ensuring the reliability of the backup power supply is essential for the safe and efficient operation of wind turbines [24].

Currently, manufacturers commonly use lead-acid batteries or supercapacitors as backup power supplies for pitch systems. However, lead-acid batteries face several drawbacks, including a short lifespan, low specific energy, and significant environmental impact. Supercapacitors, while reliable, are limited in application due to their high cost. Lithium batteries have emerged as a more suitable alternative for pitch backup power due to their mature technology and cost-effectiveness. Advances in lithium battery technology, particularly in cathode materials, have enabled higher energy densities. Lithium batteries are now available in various types, such as lithium cobalt oxide, ternary materials, lithium manganese oxide, lithium iron phosphate, and lithium titanate ($\text{Li}_4\text{Ti}_5\text{O}_{12}$). Among these, lithium titanate batteries stand out for their long lifespan, high safety, and superior performance across a wide temperature range, making them ideal for backup power applications. From an economic perspective, while the initial cost of lithium titanate battery modules is approximately double that of lead-acid batteries, they require significantly less maintenance over three years. Lead-acid batteries, on the other hand, demand annual maintenance, frequent replacements, and incur higher labor and material costs [25].

Moreover, lead-acid batteries, which are frequently utilized as backup power sources, possess a finite lifespan and demonstrate a substantial decline in capacity when exposed to low-temperature environments. At a temperature of -20°C, these batteries retain merely about 40% of their initial capacity. Also, their capacity to deliver the requisite power can be a constraining factor, necessitating replacement on an annual basis. In comparison, ultracapacitors boast a significantly extended lifespan and exhibit superior performance under extreme temperatures. However, their low energy density (3–10 Wh/kg) results in systems that are both heavy and costly. While electric double-layer capacitors (EDLCs) are durable, they typically allow only one adjustment, which increases the system's vulnerability in critical situations [24].

a) Design & Sizing

In this study it used Lithium batteries as for its advantages mentioned above. The following steps summarize the sizing for batteries back-up system.

Assumptions & Estimations:

- The calculations focus on Single Axis Calculations: calculations for one axis and could be scaled appropriately if needed.
- Emergency Stop: the emergency stop system should allow for a single full cycle of pitching from 0° to 90° to ensure safety and functionality.
- Cycle 1: Emergency stop, pitching the blade from 0° to 90°.
- Cycle 2: Repositioning the blade back to 0° for safety or maintenance.
- Pitch rates of 4°/s.

For motor data, please reference figure 4.12.

Energy Required for the motor side:

$$\text{Electrical Work} = \sqrt{3} \cdot U_N \cdot I_{max} \cdot t \cdot PF \quad (4.15)$$

Where,

U_N : Nominal motor voltage (V)

I_{max} : Maximum motor current (I)

PF: Power Factor

t : Time based on pitch rate (4°/s) = [180 (deg) / 4 (deg/sec)] · 2 = 90 sec

$$I_{max} = 39.9A \times 1.1 \text{ service factor (SF)} = 43.89A \quad (4.16)$$

$$\text{Electrical Work} = \frac{\sqrt{3} \cdot 400 (V) \cdot 90 \cdot 43.89 (A) \cdot 0.85}{3600} = 646.16 \text{ Wh}$$

Add Safety Margin (30%):

$$\text{Electrical Work} = 646.16 \text{ Wh} \cdot 1.3 = 840 \text{ Wh} \quad (4.17)$$

b) Battery Selection: Delta Battery

For the backup system, Delta Batteries were selected due to their proven reliability and suitability for various applications. Delta batteries are designed for use in demanding environments where consistent and efficient power backup is crucial.

Applications:

Energy Back-up and Storage: These batteries are ideal for providing reliable energy backup and storage solutions for residential, commercial, and industrial needs, ensuring smooth operation during power interruptions.

Direct Replacement for Conventional Lead-Acid Systems: Delta batteries are an excellent choice as a 48V direct replacement for conventional lead-acid battery systems, offering improved performance, longevity, and efficiency



Figure:- 4. 15: Delat Battery, [26]

Category	Details
Dimensions (W x H x D)	310 (± 1) x 481 (± 1) x 175.5 (± 1) mm (Without mounting kit)
Weight	Approx. 30 ± 2 kg (Without mounting kit)
Parallel Connecting Quantity	Max 6 modules in parallel in system
Materials of Enclosure	Aluminum with corrosion resistant coating
Color	Light Gray (NCS S 1002-B)
Thermal Management	Heater / Low-k thermal barrier / Solar radiant resist coatings
Mount Kit (Optional)	Ground-mounted, wall-mounted or pole-mounted

Table:-4. 5: Specification of Battery, Source [27]

- Number of Batteries

$$\frac{\text{Energy required}}{\text{Battery Capacity}} = \frac{840}{2400} = 0.35 = 1 \text{battery} \quad (4.18)$$

- Determine Series Configuration for Voltage

$$\text{Total Voltage (V)} = \text{Number of Batteries in Series} \times \text{Nominal Voltage per Battery} \quad (4.19)$$

$$\text{Number in series} = 400\text{V}/48\text{V} = 8.33 = 9 \text{ Batteries} \quad (4.20)$$

- Determine Parallel Configuration for Current

$$\text{Total Current(A)} = \text{Number of Parallel Strings} \times \text{Battery Maximum Discharge Current} \quad (4.21)$$

$$\text{Number of Parallel Strings} = 39.9\text{A}/50\text{A} = 0.798 \text{ string} = 1 \text{ string} \quad (4.22)$$

- Total batteries required:

Batteries in Series: 9

Parallel Strings: 1

Total Batteries Needed: 9

c) Inverter selection

For this system, the selected inverter is the SMA Sunny Tripower X STP 25-US-50, which meets the motor's requirements with its 400 V three-phase AC output, 25 kW power rating, and a DC input range of 430–800 V, compatible with the 432 V battery bank. Key selection parameters include ensuring the inverter matches the motor's voltage (400 V AC) and power (≥ 25 kW), accommodates the battery bank's DC input voltage, and supports the required current with high efficiency ($\geq 95\%$)



Figure:- 4. 16: Sunny Tri-Power Inverter, Source [28]

Technical data	Sunny Tripower X 20-US	Sunny Tripower X 25-US	Sunny Tripower X 30-US
Input (DC)			
Maximum array power	30000 Wp	37500 Wp	45000 Wp
Maximum system voltage		1000 V	
Rated MPP voltage range	350 V to 800 V	430 V to 800 V	515 V to 800 V
Minimum DC voltage / start voltage		150 V / 188 V	
Maximum usable operating input current / Maximum short circuit current per MPPT		24 A / 37.5 A	
MPP trackers / strings per MPPT input		3 / 2	
Output (AC)			
Nominal output power	20000 W	25000 W	30000 W
Maximum apparent power	20000 VA	25000 VA	30000 VA
Output phases / line connection		3 / 3-(N)-PE	
Nominal AC voltage		480 V / 277 V	
AC voltage range		244 V to 305 V	
Maximum output current	24 A	30 A	36 A
Rated grid frequency / range		60 Hz / -6 Hz to +6 Hz	
Power factor at rated power / adjustable displacement		1 / 0.8 leading to 0.8 lagging	
Harmonics (THD)		< 3 %	
Efficiency			
CEC efficiency	97.5 %	98 %	98 %

Figure:- 4. 17: Sunny Tri-Power Inverter, Source [28]

4.3 Blade bearing

For blade pitching to be implemented, it is essential to enable the rotor blades to rotate around their longitudinal axis. This rotational capability is essential for adjusting the blade's pitch angle, which optimizes energy capture and protects the turbine under various wind conditions. Although the required rotation angles and speeds are relatively modest, the blades are predominantly supported by bearings at their roots. [5]

Blade bearings connect to the rotor blade and the rotor hub of a wind turbine by means of bolted connections. Their rings tend to be made of steel, with 42CrMo4 type steel is the most common choice of material, whereas rolling elements are made from 100Cr6. [29]

4.3.1 Types of Bearings

The following basic design types are in commercial use as pitch and yaw rolling bearings of wind turbines:

a) Four-point contact ball bearings

Four-point contact ball bearings are the dominant type for pitch bearings bearings. For smaller turbines, they have one row; for larger turbines, usually two. Four-point contact ball bearings are generally capable of carrying loads in any degree of freedom and allow for high deformations in the interfaces.

Double row 4-point contact ball bearings utilize a point contact design that leads to high contact pressure. They have an initial contact angle of 45 degrees, which enables them to accommodate combined axial and radial loads. However, their load-bearing capacity is comparatively lower than that of triple row roller bearings, as the contact area is reduced. These bearings are prone to high bearing ring deformation and ring separation under heavy loads, which can impact their longevity. They also experience high edge loading, as the balls tend to move toward the edges of the raceway under load, increasing wear and stress. Additionally, they handle high radial loads, but this contributes to periodic ring stresses, which can lead to fatigue over time.

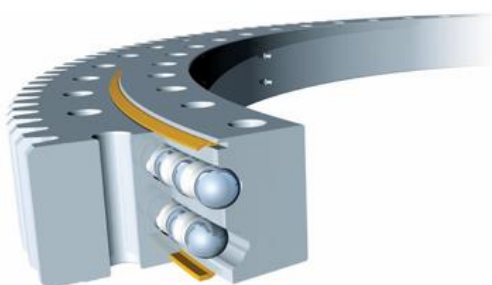


Figure:- 4. 18: Double row four-point contact ball bearing external toothed, 2024. Source [30]



Figure:- 4. 19: Double row four-point contact ball bearing internal toothed,2024. Source [30]

Apart from some disadvantages this type of bearing offers advantages such as both raceways carry the load simultaneously, enabling better load distribution and enhanced stability. Their manufacturing complexity is moderate, as their design is simpler compared to triple row roller bearings. Consequently, the manufacturing costs are comparatively cheaper, making them more economical for applications where cost is a significant factor. These bearings experience less wear due to their point contact mechanism, which reduces friction and surface stress. However, their service life is shorter when subjected to very high load applications, limiting their suitability for extreme operating conditions. [31]

b) Three-row roller bearings

The three-row roller bearing has two rows of axial roller elements that help it endure axial loads and one row of radial roller elements that help it survive radial loads. These two-row roller components aid in absorbing heavy radial loads.



Figure:- 4. 20: Three raw rollers bearing with internal toothing ,2024. Source [30]



Figure:- 4. 21: Three raw rollers bearing with External toothing,2024. Source [30]

Triple row roller bearings are characterized by a line contact design that results in low contact pressure compared to other bearing types. They have a specific contact angle configuration, with the axial row at 90 degrees and the radial row at 0 degrees, enabling better support for axial and radial loads. Due to their large contact area, they exhibit a high load-bearing capacity, making them ideal for applications requiring robust performance. Additionally, they experience low bearing ring deformation and minimal ring separation under load, enhancing their durability. Edge loading, which occurs due to roller tilt during deformation, is generally low in these bearings. Moreover, they handle radial loads effectively, with very low stress levels, due to their dedicated radial row of rollers. [32] [20]

The manufacturing complexity of these bearings is very high due to their intricate design. This complexity translates to high manufacturing costs. However, their robust design provides a high life expectancy, making them ideal for applications demanding long-term durability and reliability. This type of bearing is more compact compared to double-row four-point contact ball bearings for the same load capacity, making it well-suited for Optimus Shakti.

c) Three-row ball and roller bearings

This type of bearing is an improvement of double row four-point contact ball bearing. Three row ball and roller bearings tend to have lower radial deformations under load than four-point contact ball bearings, but they do not provide significantly higher load ratings. This is why this type of bearing is not used in large-capacity wind turbine. [32]

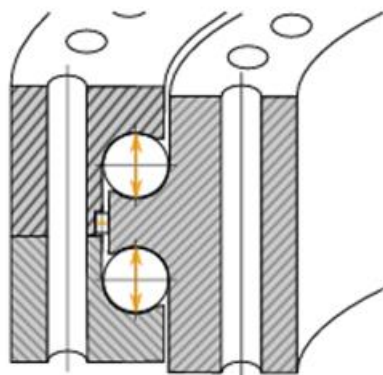


Figure:- 4. 22: Three raw ball and roller bearing,2024. Source [32]

d) Two-row angular contact bearings

Angular contact ball bearings have inner and outer ring raceways that are displaced relative to each other in the direction of the bearing axis. This means that these bearings are designed to accommodate combined loads, i.e. simultaneously acting radial and axial loads.

The axial load carrying capacity of angular contact ball bearings increases as the contact angle increases. The contact angle is defined as the angle between the line joining the points of contact of the ball and the raceways in the radial plane, along which the combined load is transmitted from one raceway to another, and a line perpendicular to the bearing axis.



Figure:- 4. 23: Double row angular contact ball bearing,2024.Source [33]

While they perform well under combined loads, their load capacity is lower than that of larger, more robust designs like triple-row roller bearings. This limits their use in very large-capacity wind turbines. The point contact design leads to higher localized stress, which can result in increased wear and reduced service life under extreme loading conditions. [32]

4.3.2 Blade attachment

The connection of Wind turbine blades with the hub can be possible via two different concepts, inner rotating and outer ring rotating. Each choice has its own advantages and disadvantages. Many aspects influence the decision, such as the cost of the surrounding parts, assembly processes, Maintenance accessibility and technical feasibility, this is a very important step, which will again influence the further design of the Hub.

4.3.2.1 Outer ring Rotating

In this configuration, the blade is attached to the outer ring of the pitch bearing, while the inner ring is fixed to the hub. This design offers several advantages, such as enabling a smaller and lighter hub, simplifying the connection of the lubrication system to the blade bearing, and creating additional space within the hub.

However, a significant drawback is the increased risk of blade detachment if the bearing cracks, posing serious safety concerns.



Figure:- 4. 24: Outer Ring mounted blade,2024.Source [34]

Additionally, since pitch system are located outside the hub, extra protective measures, such as a spinner and additional support structures (teeth cover), are necessary to shield these components from environmental exposure. [29]

4.3.2.2 Inner ring Rotating

As the name suggests, this configuration involves the blade being mounted on the inner ring, while the outer ring is fixed to the hub. This setup allows for a stiffener plate to be placed between the inner ring and the blade without requiring additional components, enhancing the structural stiffness of the bearing. Furthermore, in the event of a ring crack, the likelihood of blade detachment is significantly reduced.

During turbine assembly, blade bolts can be tightened from within the hub, making the process more convenient compared to external configurations.

Additionally, the pitch drives are housed within the hub, eliminating the need for extra housing and simplifying maintenance tasks.



Figure:- 4. 25: Inner Ring mounted blade,2024.Source [10]

The inner ring configuration also benefits from a larger diameter, allowing for the inclusion of more rolling elements. This design ensures better load distribution and reduces the forces on individual rolling elements if the moment remains constant. [29]

In summary, the choice between inner and outer ring configurations depends on multiple factors. While the outer ring design offers a more compact structure, it is less favorable for maintenance and the safety of components and technicians. Conversely, the inner ring design prioritizes durability, ease of maintenance, and safety, making it the preferred choice for the Optimus Shakti turbine.

4.3.3 Dimensioning of the Three row roller bearing

The statical calculations aim to ensure that the blade bearing can withstand the maximum load situations occurring for all operating conditions of the turbine.

The calculation starts with the analysis of the load time series for the DLCs in order to identify the maximum resulting bending moment.

The dominant load of a pitch bearing is the resulting moment (M_{xy}) Which is the combination of flap-wise and edge-wise bending moment.

$$M_{xy} = \sqrt{M_x^2 + M_y^2} \quad (4.23)$$

Radial (F_z) and Axial (F_{xy}) forces influence the rolling body loads as well

The following loads taken for the calculation (cf. Section 3-Loads)

Bending Moment $M_{xy} = 40000 \text{ kN/m}$

Radial force (F_z) = 800 kN

Axial force (F_{xy}) = 900 kN

Assumption for the Calculations:

The upper and lower axial raceways have the same raceway diameter D_{pw} , [mm]

The upper and lower axial raceways have the same roller diameter D_w [mm]

Roller length L [mm] = roller diameter D [mm]

The radial raceway is not considered

Calculation of Hertzian pressure

For the calculation of the Hertzian pressure we followed procedure as given by our supervisor.

- Define raceway system parameters (D_{pw} , D_w , L and Z)

Set raceway diameter D_{pw} [mm]

For calculating D_{pw} (bearing raceway diameter), bolt circle diameter D_{bcd} need to consider. Which was 3600 mm, given by the Blade team.

$$D_{pw} = D_{bcd} + (2*W3) + (2*S_u) + (WA-L) + L = 3801 \text{ mm} \quad (4.24)$$

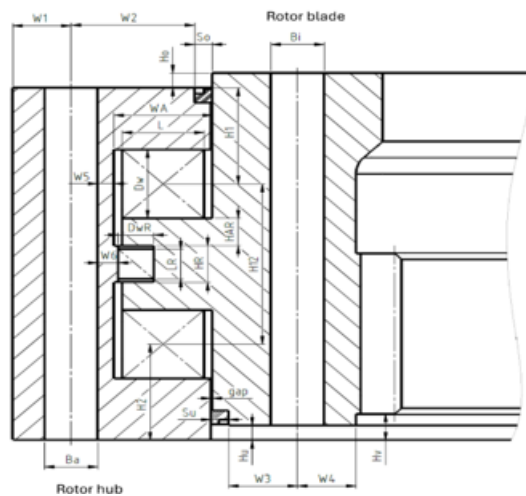


Figure:- 4. 26: Three rows roller bearing,2024.Source. [4]

Set roller diameter D_w [mm]

Roller diameters up to 80 mm would theoretically be possible (from raceway surface hardening point of view). However, the length of the rollers can cause large bearing ring deformations. Therefore, roller diameters greater than 65 mm should be avoided.

Use roller diameters 50, 55, 60, 65 mm.

$$D_w = 65 \text{ mm}$$

Roller length L [mm] = roller diameter D_w [mm] = 65 mm

Estimate number of rollers per axial raceway Z for the given D_{pw} and D_w :

$$Z = \frac{\pi * D_{pw}}{D_w * 1.15} = 160 \quad (4.25)$$

- Calculate maximum roller force (Q_{\max})**

Maximum roller force for ideal conditions (rigid companion structure, same stiffness over the entire bearing circumference): [4]

$$Q_{\max_rigid} = \frac{F_z}{Z} + \frac{4.1 * M_{xy}}{D_{pw} * Z} = 274.67 \text{ kN} \quad (4.26)$$

The influence of the companion structure can be considered by an additional factor K_q : and For good rotor blade and rotor hub designs: $K_q \leq 1.15$. [4]

$$Q_{\max_flexible} = K_q * Q_{\max_rigid} = 315.87 \text{ kN} \quad (4.27)$$

The highest contact force Q_{\max} obtained which is used to calculate the highest resulting Hertzian pressure p_{\max} .

- Calculate maximum contact stress (p_0)**

The Hertzian calculations cannot be solved analytically. Hence, equations for an approximation were well established. For example, Houpert published a method. The maximum pressure (p_{\max}) follows according to 3.3, the Hertzian contact ellips radii are required inputs for the equation. Here, another iterative process comes into play. [32]

$$b = 0.00335 * \sqrt{\frac{Q_{\max_flexible}}{L_{we} * \sum \rho}} = 1.37 \quad (4.28)$$

$$L_{we} = L - (2 * r_{\text{axial}}) = 61 \text{ mm} \quad (4.29)$$

$$p_{0\max} = \frac{2 * Q_{\max_flexible}}{\pi * b * L_{we}} = 2398.72 \text{ N/mm}^2 \quad (4.30)$$

Due to bearing ring deformation, the rollers tilt leading to an uneven pressure distribution and thus higher contact stresses. This can be considered by an additional factor K_p : For stiff bearing design, $K_p \leq 1.20$. [4]

$$p_{\max} = p_{0\max} * K_p (1.20) = 2878.47 \text{ N/mm}^2 \quad (4.31)$$

According to ISO 76, Permissible contact stresses shall be less than 4.2 GPa for ball bearings and 4.0 GPa for roller bearings. However, since these pressures are related to extreme wind conditions, typical contact pressures during normal operation of the turbine are lower. However, when using the criterion 3300 N/mm^2 , it is likely that the bearing is also feasible for the fatigue loads.

4.3.4 Pitch bearing safety factors calculation

The load limit for gear wheels is determined by the load capacity. According to DIN 3979, there are three main types of damage to gears that determine the load limit:

- Tooth breakage due to excessive bending stress in the tooth root,
- Tooth flank fatigue due to material fatigue (pitting, chipping),
- Scuffing due to the combined effect of pressure and sliding speed.

Tooth breakage typically refers to the complete or partial fracture of a tooth when its load-bearing capacity is surpassed. To prevent this, the safety and integrity of the tooth root must be evaluated.

Fatigue on tooth flanks appears as pitting when the contact pressure exceeds the tolerable limit. Repeated loading and unloading cause material fatigue, leading to pits after numerous rollovers. This is critical only if pitting worsens with service life or pits grow larger, indicating diminished load capacity due to exceeded permissible flank pressure, so the load capacity of the tooth flank needs to be checked. [35]

- **Maximum forces**

By given Maximum torque of 612 kNm , the tangential force on the gear teeth can be calculated, as follows: [35]

$$F_{t,12} = \frac{2*T_{max}}{d_2} = 355 \text{ kN} \quad (4.32)$$

where,

d_2 = effective diameter of pitch bearing gear teeth,

$m_n * Z_2 = 3440 \text{ mm}$,

This Tangential force is divided into two components as shown in fig, the normal tooth force F_b (perpendicular to the flank and mating flank at the point of contact) and the radial force (always directed towards the respective wheel center) F_r .

Since α is the same as (20°) these forces can be calculated with the following equations : [35]

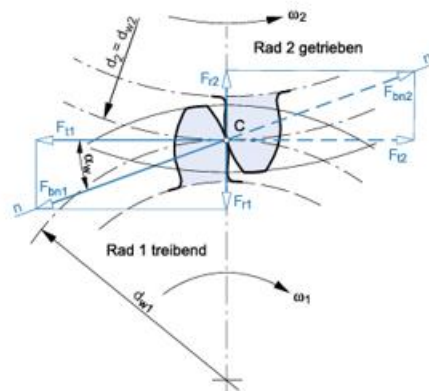


Figure:- 4. 27: Forces on Gear ,2005.Source [35]

Normal tooth force [35]

$$F_{bn12} = \frac{F_{t1,2}}{\cos\alpha} = 378.6 \text{ kN} \quad (4.33)$$

Radial force [35]

$$F_{rn12} = F_{t1,2} * \tan\alpha = 129.5 \text{ kN} \quad (4.34)$$

Nominal forces:

With the given nominal torque of 250 kNm per pitch system the tangential force on the gear can be calculated by the following equation. [35]

$$F_{t,12_nomi} = \frac{2*T_{nomi}}{d_2} = 145.34 \text{ kN} \quad (4.35)$$

Stress Influencing Factors

For practical design, simplified methods (C & D) are often used as most industrial gearboxes operate in the subcritical range, ensuring faster calculations with sufficient accuracy.

The application factor (operating factor) K_a , accounts for external additional forces specific to the input and output machines connected to the gearbox. These forces include shocks, torque fluctuations, and load peaks. [35]

$$K_a = 1 \quad (4.36)$$

Dynamic factor K_v , it records the internal dynamic additional forces that arise under load due to deformation of the teeth wheel center and all other force-transmitting elements of the gearbox. [35]

$$K_v = 1 + \left(\frac{K_1}{\frac{F_{t12_nomi}}{b} * K_a} + K_2 \right) * K_3 = 1 \quad (4.37)$$

Where,

$$K_1 = 24.5; \text{ Gear quality 8 considered}$$

$$K_2 = 0.0193$$

$$K_3 = 0.01 * Z_1 * V_t * \sqrt{\frac{u^2}{1+u^2}} = 0.0062 \quad (4.38)$$

Face width factors

Face width factors " $K_{H\beta}$ " and " $K_{F\beta}$ " They take into account the effects of uneven force distribution over the tooth width on the flank stress (' $K_{H\beta}$ ') or on the tooth root stress (' $K_{F\beta}$ '). This is caused by the flank line deviations that occur in the loaded state as a result of mounting and elastic deformations (F_{sh}) and manufacturing deviations (F_{ma}). [35]

$$K_{H\beta} = 1 + \frac{10 * F_{\beta y}}{\left(\frac{F_{tnomi}}{b}\right)} = 1.3 \quad (4.39)$$

Taking into account the following influencing variables:

F_{sh}) Flank line deviation due to deformation can be determined as a first approximation from experience. [35]

$$F_{sh} = 0.023 * \left(\frac{F_{tnomi}}{b}\right) * \left[\left| 0.7 + K' * \left(l * \frac{s}{d_1^2} \right) * \left(\frac{d_1}{d_{sh}} \right)^4 \right| + 3 \right] * \left(\frac{b}{d_1} \right)^2 = 5.39 \mu m \quad (4.40)$$

Where,

$$d_1 = \text{pitch circle diameter of pinion} = 256 \text{ mm}$$

$$b = \text{tooth width} = 162.5 \text{ mm}$$

$$\left(\frac{F_{tnomi}}{b}\right) = K_v * (K_a * F_t / b) = 894 \text{ N/mm}$$

Now, we have to find F_{ma} . is production related flank line deviation as below, [35]

$$F_{ma} = c * 4.16 * b^{0.14} * q_H = 21.97 \mu m \quad (4.41)$$

Where ,

$c = 1$ for wheel pairs without adjustment measures

$$q_H = 2.59,$$

Effective flank line deviation before running-in [35]

$$F_{\beta X} = F_{ma} + 1.33 * F_{sh} = 29.14 \mu m \quad (4.42)$$

This amount is reduced by the run-in amount 'y' according to TB 21-17, so that after the run-in the effective flank line deviation is [35]

$$F_{\beta Y} = F_{\beta X} - y_b = 23.14 \mu m \quad (4.43)$$

Where,

$$y_b = 6$$

The exponent for determining the width factor for the tooth root results from [35],

$$N_f = \frac{\left(\frac{b}{h}\right)^2}{1 + \left(\frac{b}{h}\right) + \left(\frac{b}{h}\right)^2} = 0.81 \quad (4.44)$$

When this is done, the tooth base width factor is calculated [35]

$$K_{F\beta} = K_{H\theta}^{N_f} = 1.24 \quad (4.45)$$

Next values for the face load factor $K_{H\alpha}$ and $K_{F\alpha}$ are assumed according to [35], with the tooth quality of 8 and regular straight gears [35]

$$K_{H\alpha} = K_{F\alpha} = 1.1 \quad (4.46)$$

With all these values the total influence factors K_{Fges} (tooth base strength factor) and K_{Hges} (tooth flank/pitting factor) are determined [35]

$$K_{Fges} = K_a * K_v * K_{F\alpha} * K_{F\beta} = 1.36 \quad (4.47)$$

$$K_{Hges} = \sqrt{K_a * K_v * K_{H\alpha} * K_{H\theta}} = 1.20 \quad (4.48)$$

The maximum local tooth root stress occurring when a fault-free gear is loaded by the static nominal torque can be determined from

$$\sigma_{f01} = \frac{F_{t12\text{nomi}}}{b*m_n} * Y_{fa} * Y_{sa} * Y_{\epsilon} = 164.14 \text{ N/mm}^2 \quad (4.49)$$

Where,

Y_{fa} = 2.42 (Form factor)

Y_{sa} = 1.82 (Stress correction factor)

$Y_{\epsilon} = 0.25 + \frac{0.75}{\varepsilon_{\alpha}} = 0.6667$ (Overlap Factor)

Total tooth root stress can be calculated as follows,

$$\sigma_{f12} = \sigma_{f01} * K_{Fges} = 223.50 \text{ N/mm}^2 \quad (4.50)$$

Tooth root limit strength can be calculated by,

$$\sigma_{fg1} = 2 * \sigma_{flim} * Y_{NT} * Y_X = 642.06 \text{ N/mm}^2 \quad (4.51)$$

Where,

σ_{flim} = 369 N/mm² for Bearing and 500 N/mm² for the Pinion

Y_{NT} = 1 (Service life factor)

Y_X = 0.87 (Size Factor)

Safety of the tooth root load capacity

$$S_{f1} = \frac{\sigma_{fg1}}{\sigma_{f1}} = 2.87 \quad (4.52)$$

Verification of pit load-bearing capacity

The calculation of the pitting load-bearing capacity is based on the flank pressure σ_H at the rolling point, and the flank pressure that occurs at the rolling point is [35]

$$\sigma_{H0} = Z_H * Z_E * Z_{\epsilon} * Z_B * \sqrt{\left(\frac{u+1}{1}\right) \left(\frac{F_1}{b*d_1}\right)} = 755.17 \text{ N/mm}^2 \quad (4.53)$$

Where,

Z_H is zone factor, takes into account the flank curvature at the rolling point, which is 2.5 for straight gears.

Z_E is Elasticity factor, which is 189.8 N/mm^2

Z_ε is Coverage factor, takes into account the influence of the load distribution on several pairs of flanks involved in the engagement on the calculated Hertzian pressure, which is 0.825

Z_β is Screw factor, it records the improvement in load-bearing capacity under flank pressure with increasing helix angle, which is 1.

flank pressure occurring at the rolling circuit is [35],

$$\sigma_H = \sigma_{H0} * K_{Hges} = 903.18 \text{ N/mm}^2 \quad (4.54)$$

flank limit strength

Flank limit strength can be determined by the following equation [35]

$$\sigma_{HG} = \sigma_{Hlim} * Z_{NT} * Z_L * Z_V * Z_R * Z_W * Z_X = 1743.20 \text{ N/mm}^2 \quad (4.55)$$

Where,

σ_{Hlim} is tooth flank fatigue strength, 1204.44 N/mm^2

Z_{NT} is Service life factor, takes into account a higher permissible pressure if a limited service life is required in timing gears, which is 1.

Z_L is Lubricant factor, for mineral oils depending on the nominal viscosity at 50° or 40° , which is 1.

Z_V is Velocity factor, takes into account the influence of the circumferential speed on the flank load-bearing capacity, which is 0.89

Z_R is Roughness factor, determines the influence of surface roughness, which is 0.87

Z_W is Material pairing factor, takes into account the increase in flank strength of a gear made of structural steel, heat-treated steel, which is 1.

Z_X is Size factor, calculates the influence of the tooth dimensions, which is 0.87

Safety of the flank load capacity

$$S_{H12} = \frac{\sigma_{HG}}{\sigma_H} = 1.93 \quad (4.56)$$

4.3.5 CAD model of Bearing and dimensions

Pitch Bearing	
Bearing type	Triple row roller bearing
Inner BCD of Bearing	3600 mm
Outer BCD of Bearing	4006 mm
Bolts on inner BCD	140*M36
Bolts on outer BCD	145*M39
Material	42crM04
Weight	8 T
Height	338 mm
Outer Diameter	4125 mm

Table:-4. 6:- Specification of Pitch Bearing of Optimus Shakti



Figure:- 4. 28: CAD modele of Three row roller bearing of Optimus shakti

4.4 Bolted Connection between Hub and Shaft

The hub and shaft are connected by a bolted joint, these bolts experience axial, lateral, bending and torsional loads from static, periodic, and random forces. The goal is to calculate the loads on each screw to identify the most stressed one, ensuring safety and reliability. The diagram illustrates these forces and moments on the rotor flange and its connection.

Calculating loads on screws is essential to prevent overloading, optimize their design, and identify potential failures early for effective maintenance. [9]

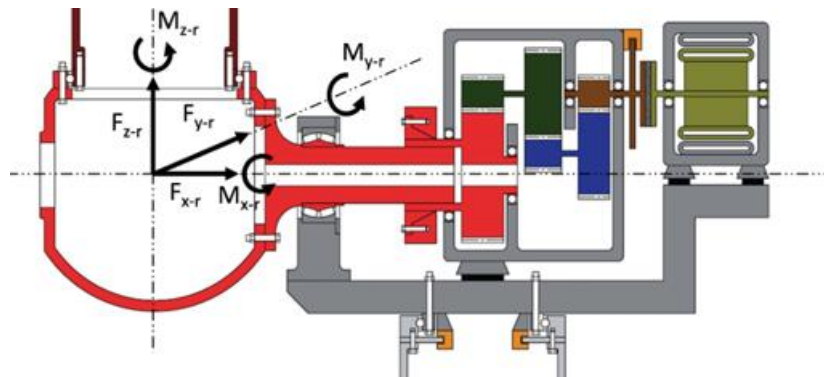


Figure:- 4. 29:- Loads on bolts on Rotor flange connection,2024.Source [9]

Now, there are different concepts for bolted connection as shown in fig.

The design A provides increased capacity to handle torque and bending moments, allows for easy installation from the nacelle, requires machining of only one flange, and ensures an optimal flow of forces for improved structural efficiency.

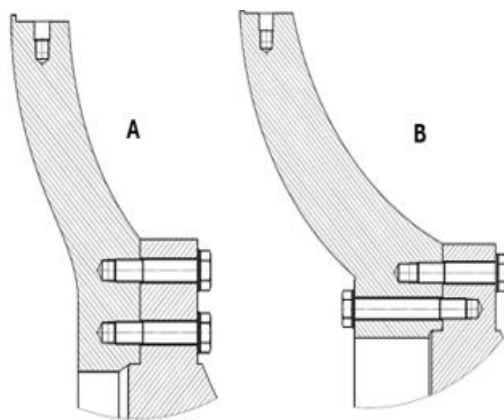


Figure:- 4. 30: 1 Rotor flange connection,2024.Source [9]

The advantage of design B is that it allows smaller bolt circle diameters; however, the primary drawback of design B is that the internal flange requires machining, and installation is only possible from the hub side, increasing handling effort.

Therefore, we have chosen concept A for Optimus Shakti. [9]

Calculation of Bolted Joint

Assuming specific conditions for calculation such as, the flange must be rigid to minimize deformations and prevent connection skidding, with screws designed to function without pre-stressing.

Axial Force	Lateral Force	Bending Moment	Torsional Moment
$F_{a_f_ges}$	$F_{q_f_ges}$	M_b	M_t
700 kN	2000 kN	25000 kNm	12000 kNm

Table:-4. 7: 1 Loads for Bolted joint varification, Section:-3

And the Following data considered for bolted joint verification, given by our supervisor Mr. Christian Bulligk.

Inner BCD	Outer BCD	No. of bolts (inner BCD)	No. of bolts (Outer BCD)	Size of Bolts	Co-efficient of Friction
BCD _{in}	BCD _{out}	N _{s_{in}}	N _{s_{out}}	M39	μ
2.140 m	2.340 m	56	60	39 mm	0.3

Table:-4. 8: initial data considered for the Bolted joint verification

Step 1: Total Shear force on bolt by Torsion and Lateral forces (F_{q_ges})

Shear force on Bolt by External Lateral Force

$$(F_{qF}) = \frac{F_{q_f_ges}}{N_{s_{in}} + N_{s_{out}}} = 17.24 \text{ kN} \quad (4.57)$$

Shear Force on screw by torsional moment

$$(F_{q_mt_max}) = \frac{r_{tmax} * M_t}{N_{s_{in}} * r_{t_1}^2 + N_{s_{out}} * r_{t_2}^2} = 96 \text{ kN} \quad (4.58)$$

Where,

r_{tmax} = Outmost screw circle diameter, 1.170 m

r_{t_1} = BCD_{in}/2 = 1.07 m

r_{t_2} = BCD_{out}/2 = 1.17 m

Total Shear force on bolt by Torsion and Lateral forces (F_{q_ges})

$$F_{q_ges} = F_{qF} + F_{q_mt_max} = 113.24 \text{ kN} \quad (4.59)$$

Step 2: Total axial force on bolt by bending moment and Tensile force (F_{a_ges})

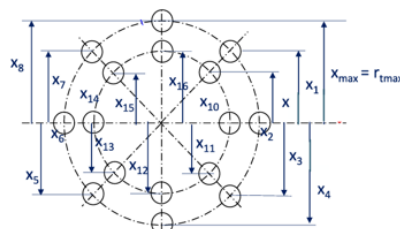


Figure:- 4. 31: Distance of bolts to bending axis,2024.Source [9]

Axial force on bolt by Bending moment

$$(F_{a_mb_max}) = \frac{X_{max} * M_b}{\sum_{i=1}^{n_{SB}} X_i^2} = 400.00 \text{ kN} \quad (4.60)$$

Where,

$$X_{max} = r_{tmax}$$

X_i = Distance of the perpendicular screw to the bending axis [m]

n_{SB} = Total number of Screws

Axial force on bolt by tensile force

$$(F_{a_zd}) = \frac{F_{a_zd_ges}}{N_{S_{in}} + N_{S_{out}}} = 6.03 \text{ kN} \quad (4.61)$$

Total axial force on bolt by bending moment and Tensile force (F_{a_ges}) =

$$F_{a_ges} = F_{a_mb_max} + F_{a_zd} = 406.03 \text{ kN} \quad (4.62)$$

Step 3: Required area of bolts for carrying total load A_req

First, we have to calculate

$$F_{clamp} = \frac{F_{q_ges}}{\mu} = 377.49 \text{ kN} \quad (4.63)$$

Total force on bolts is summation of total axial force and clamping force

$$F_{total} = F_{a_ges} + F_{clamp} = 783.53 \text{ kN} \quad (4.64)$$

Now, the bolt diameter required for the design of the screw connection can be calculated by,

$$A_s = \frac{F_{total}}{R_{p02}} = 833.55 \text{ mm}^2 \quad (4.65)$$

Where, R_{p02} = proof stress of the screw material

So, $A_{req}(835.64 \text{ mm}^2)$ is < A_{s_M39} (976 mm^2 from (Source [35] TB 08-1, p. 1127) So, the design is safe

4.5 Bolted connection between Bearing and Hub

The blade is attached to the hub flange using a bolted connection. This connection must provide a secure and permanent bond capable of withstanding the dynamic and ultimate loads throughout the turbine's service life. Additionally, the bolted connection facilitates the preloading of the rolling elements in the three-row roller bearing.

The preliminary design for the outer ring follows an iterative approach to balance various requirements. The initial step in defining the bolted connection design involves determining the number of bolts. This number should be based on the available space and the ultimate loads expected to be carried by the bearing flange. [29]

$$N = \frac{\pi D}{2.2 \cdot d} = 147 \text{ Number of bolts} \quad (4.66)$$

Where,

D = bolt circle diameter of Bearing outer ring = 4006 mm

d = bolt diameter = 39 mm (M39 bolts)

The number of bolts is determined by the space required for tightening tools, such as hydraulic torque wrenches or bolt tensioners. This design uses 145 bolts, resulting in an approximate 87 mm spacing on the outer ring, which appears adequate.

Following are the Loads are given by the supervisor, (cf- section 3)

Axial load (F_{ax}) = 800 kN

Radial load (F_{xy}) = 900 kN

Resulting bending moment based on blade bottom coordinate (M_{xy}) = 40000 kNm

Bolt circle diameter of the outer race of pitch bearing (D_{out_bcd}) = 4006 mm

The ultimate loads acting on the flange have to be transferred into an axial force carried by the bolts. [9]

$$F_b = \left(\frac{F_{ax}}{n_b} + \frac{2 \cdot M_{xy}}{r \cdot n_b} \right) = 280.96 \text{ kN} \quad (4.67)$$

The clamping force needed to provide enough resistance against the opening of the contact can be estimated as follows

$$F_k = s * F_b = 337.16 \text{ kN} \quad (4.68)$$

The factor s is set to 1.2, which is typical for dynamic load situations. In general, the clamping force F_K should be higher than the working load F to ensure a positive residual clamping load. Both loads are used to estimate the stress cross section needed for the bolted connection.

This estimation needs values such as, K_a determines a factor for the tightening method, K is a reduction factor based on the type of bolt, β a factor for the elastic resilience of the used bolt, E the Young's modulus for steel, f_z a factor for embedding, l_k the clamping length and $R_{p,02}$ the proof stress of the used bolt. For the preliminary design in this section, the following values are chosen according to reference. [9]

$$R_{p,02} = 900 \text{ MPa} \text{ according to bolt type 10.9}$$

$$K_a = 1.2 \text{ Hydraulic tensioning}$$

$$K = 1.15 \text{ for the shank screws}$$

$$f_z = 0.011, \text{ Axial load related factor}$$

$$\beta = 1.1 \text{ for shank screws}$$

$$l_k = 450 \text{ mm, length of clamped part (initial estimate)}$$

$$E = 210 \text{ MPa, Young's modulus for steel } [N/mm^2]$$

Based on the values estimated for this preliminary design, the needed stress cross section according to (3.5.4) is, [9]

$$A_s = \frac{F_b + F_k}{\left(\frac{R_{p,02}}{k \cdot k_A}\right) - \beta \cdot E \cdot \frac{f_z}{l_k}} \quad (4.68)$$

$$A_s = 956.07 \text{ mm}^2$$

The stress cross section of the bolt used shall be equal or larger than the one estimated with (3.2.4). The calculated area A_s is 956.07 mm^2 is smaller than the cross-sectional area of M39 bolts (976 mm^2 [35], so they seem to be sufficient. Therefore, the preliminary design of the bolted connection between the outer ring of the bearing and the hub shall consist of **145** bolts of the size **M39**.

4.6 Lubrication System

In wind turbines, pitch systems rely on specialized bearings to ensure precise motion and durability. Pitch systems use three-rows roller bearing, which are selected based on the rotor blade size. These bearings experience fluctuating loads and irregular operation, making proper lubrication essential to minimize wear, prevent overheating, and ensure smooth operation. Effective lubrication maintains bearing performance, improves reliability, and reduces maintenance costs, which are critical to turbine efficiency and longevity. [36]

Applying the right amount of lubricant at the right intervals is critical because both inadequate and excessive lubrication can lead to premature bearing failure and costly machine downtime. In fact, inadequate lubrication is responsible for approximately 36% of all bearing failures, underscoring the importance of accurate lubrication practices. [37] This chapter focuses on calculating the grease quantity and relubrication interval for bearings based on the guidelines provided in the SKF Maintenance Handbook. The calculations will ensure optimum lubrication to maximize bearing performance and life while minimizing downtime and maintenance costs.

4.6.1 Manual vs. Automatic Lubrication

Aspect	Manual Lubrication	Automatic Lubrication
Mechanism	Grease applied manually, bearings must be stationary for safety	Grease supplied via pump and distributor while turbine operates
Advantages	Sufficient for raceways	Allow continuous operation Ensure even grease distribution Improves safety by minimizing manual intervention
Disadvantages	Gear lubrication may be inadequate (Grease pushed out of contact areas) Time consuming and labor-intensive Uneven grease distribution	

Table:-4. 9:- Manual Vs. Automatic Lubrication, 2025. Source:- [38]

4.6.2 Type of automatic lubrication systems

System Type	Advantages	Disadvantages
Progressive Distributor	-Simple, robust, economical. -Good monitoring. -Flexible sizes and configurations. -Supports various lubrication types.	-Residual pressure during downtime causes oil-thickener separation, leading to leaks and inconsistent lubrication.
Injector Lubrication	- Simultaneous dispensing. - Complete pressure release when idle.	Expensive Requires more components.

Table:-4. 10: Type of Lubrication system, 2025. Source:- [38]

In our design, we selected a progressive distributor for the lubrication system due to its simplicity, robustness, and cost-effectiveness. This system allows for reliable monitoring of lubricant flow, ensuring consistent performance. Its flexible sizes and configurations make it adaptable to various design requirements, while its compatibility with different types of lubricants enhances versatility. The progressive distributor plays a crucial role in maintaining optimal lubrication and ensuring the durability of critical components.

4.6.3 Grease Volume Calculation and Grease Type Selection

Accurate grease volume calculation ensures optimal lubrication of pitch bearings. The following outlines the grease requirements for the bearing raceway and pitch bearing gear.

Annual Grease Requirement

- Bearing Raceway: The raceway can hold 31.25 kg of grease (80% of free volume), with 15.63 kg recommended for annual relubrication.
- Pitch Bearing Gear: Requires 5 kg of grease per year.
- Total Annual Requirement

$$:(15.63\text{kg} + 5\text{kg} = 20.63\text{kg/year})$$

Grease Volume for Maintenance Interval

For a 7-month operational period:

- Monthly Consumption $\left(\frac{20.63\text{kg}}{12} = 1.72\text{kg/month}\right)$:
- Grease for 7 Months: $\left(\frac{1.72\text{kg}}{\text{month}} * 7 = 12.04\text{kg.}\right)$

For 3 Bearings: $(12.04\text{kg} \times 3 = 36.12\text{kg.})$

4.6.4 Typical Grease Types for Pitch Bearings

The performance and longevity of pitch bearings heavily rely on the selection of suitable lubricants. Commonly recommended greases for pitch bearings include:

Fuchs Gleitmo 585 K / 585 K Plus

Klüberplex BEM 41-141

Mobil SHC Grease 461 WT

Selected Grease: Fuchs Gleitmo 585 K Plus

For this design, **Fuchs Gleitmo 585 K Plus** was chosen due to its compatibility with progressive distribution systems and superior performance under demanding conditions.

Key Characteristics:

Operating Temperature Range: -45°C to +130°C

Offers extensive wear protection, even under shock loads and oscillating movements.

Reduces fretting corrosion and provides excellent corrosion resistance.

Enables long lubrication intervals and is highly resistant to aging.

Ensures functional reliability of highly stressed machines and systems. [39]

GLEITMO 585 K PLUS is a high-performance lithium soap paste based on synthetic oil. It incorporates a synergistic combination of white solid lubricants designed to dampen shock loads, reduce wear, and prevent fretting corrosion. Its robust formulation allows for extended lubrication intervals, making it ideal for demanding applications like pitch bearings in wind turbines.

This selection ensures optimal lubrication performance and contributes to the reliability and efficiency of the lubrication system.

4.6.5 Lubrication Pump and Reservoir Calculation

The lubrication system for the pitch bearings is designed based on the grease density of **0.9 kg/L** to meet the relubrication requirements over a 7-month period.

Total Tank Volume Calculation:

$$\text{Total Grease Volume} = \left(\frac{36.12\text{kg}}{0.9\text{kg/L}} = 40\text{L} \right) \quad (4.69)$$

A **40 L tank** is required to meet the lubrication needs for three pitch bearings during the 7-month period

The **Compact P 653 M** was selected for the system due to its robust design and ability to handle high-demand applications.

Key Features:

Reservoir Capacity: Up to 100 liters (26.4 gallons), exceeding the required capacity for extended lubrication cycles.

Pump Elements: Supports up to three pump elements, ensuring efficient grease distribution to multiple lubrication points.

Durability: Designed for industrial use, providing consistent and automated lubrication for high-performance systems.

This pump ensures reliability and efficiency in maintaining optimal lubrication for the pitch bearings throughout the operational period.

Technical data	
Function principle	electrically operated piston pump
Operating temperature	-40 to +70 °C; -40 to +158 °F
Operating pressure	350 bar; 5 075 psi
Lubricant	grease; up to NLGI 2
Outlets	up to 3 pump elements
Metering quantity	depending on pump element; 8 cm³/min; 0.48 in³/min max. 24 cm³/min; 1.44 in³/min
Lubricant output ¹⁾	4, 8, 10, 15, 20, 30 ²⁾ ; 40 ²⁾ and 100 ²⁾ ; 1.05, 2.11, 2.64, 3.96, 5.28, 7.92 ²⁾ , 10.56 ²⁾ and 26.4 ²⁾ gal
Reservoir	G 1/4
Connection main line	90–264 V AC, 50/60 Hz; 24 V DC
Operating voltage	IP 6K 9K
Protection class	UL/CSA, CE
Approvals	min. 240 × 235 × 415 mm
Dimensions	max. 500 × 500 × 1 064 mm min. 9.45 × 9.25 × 16.94 in max. 19.69 × 19.69 × 41.89 in
Mounting positions: with stirring paddle with follower plate	reservoir upside any

Figure:- 4. 32 Lubrication Pump



Figure:- 4. 33: Lubrication Pump

4.6.6 Lubrication Pinions

Lubrication pinions are essential tools designed to apply grease uniformly across the entire tooth flank of gears. Made from durable materials such as aluminum or rubber-based composites, they ensure consistent and efficient lubrication. These pinions are commonly used in critical applications like yaw and pitch bearing teeth, where one or more lubrication pinions work together to maintain smooth operation and reduce wear. Lubrication Pinions Selection: LP2 Lubrication pinion from SKF.

Technical data	
Material	Polyurethane (PU)
Admissible material pairing of LP2 and the component to be lubricated	PU / metal
Number of teeth	8
Modules	12, 14, 16, 18, 20, 22, 24
Lubricants	Greases up to NLGI 2 ¹⁾
Max. admissible volume flow	2,0 l/min ²⁾
Lubricant inlet connection	G1/8
Operating temperature	-30 to +70 °C
Rotating direction	any
Mounting position	any
Max. speed	80 r/min
Deviation of the alignment of the axis of the lubrication pinion and the component to be lubricated	± 1 °
Maximum eccentricity of the component to be lubricated	1 mm
Active lubricant duct	in direction of arrow (indicated on the bracket)
Long-term usage / interval usage	yes / yes
Durability	min. 1 million revolutions

Figure:- 4. 34: SKF Technical data,2024 [40]



Figure:- 4. 35: Lubrication and pitch pinion assembly, 2024, Source [41]

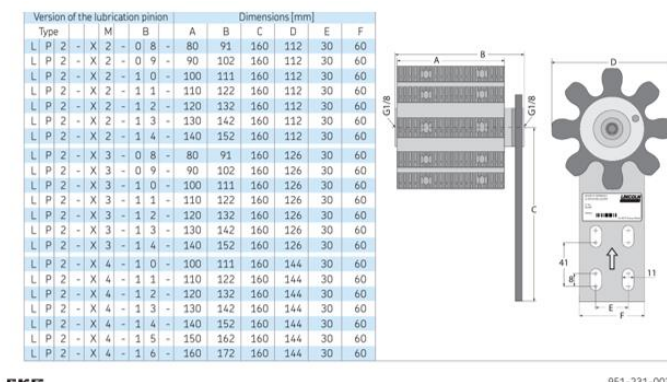


Figure:- 4. 36: Lubrication Pinion, Source [40]

4.7 Spinner

A spinner is a structural element mounted on a wind turbine's hub, covering both the hub and the inner cylindrical sections of the rotor blades. Its design, often spherical or paraboloidal, is streamlined to reduce aerodynamic drag and improve efficiency.

Spinners are typically made from lightweight, durable materials like carbon fiber or fiberglass. These materials provide strength, resistance to environmental factors such as corrosion, and ensure the spinner maintains its structural integrity while keeping the turbine lightweight.



Figure:- 4. 37: Spinner Optimus Shakti



Figure:- 4. 38: Spinner Optimus Shakti

Requirements of Spinner

Improved aerodynamics and performance

A spinner, shaped either spherically or paraboloidal, promotes smooth airflow around the hub and directs wind towards the profiled sections of the rotor blades. This design minimizes turbulence and maximizes the efficiency of wind energy capture.

Improved lifespan of Components

India experiences extreme weather conditions, particularly during the summer when temperatures can soar to around 40 degrees Celsius, and the monsoon season brings heavy rainfall. Consequently, it is essential to safeguard electrical components from these outdoor weather conditions to enhance their lifespan and reduce the occurrence of breakdowns.

Spinner protects the hub, internal components, and blade attachments from environmental factors such as debris, rain, and corrosion, enhancing their longevity and reliability.

Enhance Safety of Technician

The spinner improves technician safety by enclosing the hub and internal components, limiting exposure to moving parts and harsh weather conditions. Its streamlined design reduces risks by preventing debris and ice buildup. Furthermore, it facilitates easier and safer access for maintenance and inspections.

Aesthetics

The spinner improves the aesthetics of wind turbines by providing a sleek, streamlined design that integrates smoothly with the turbine's overall look. Its clean and modern appearance reduces visual disruption, making turbines more visually appealing in both urban and scenic settings.

4.8 Complete Assembly for Rotor hub and pitch system

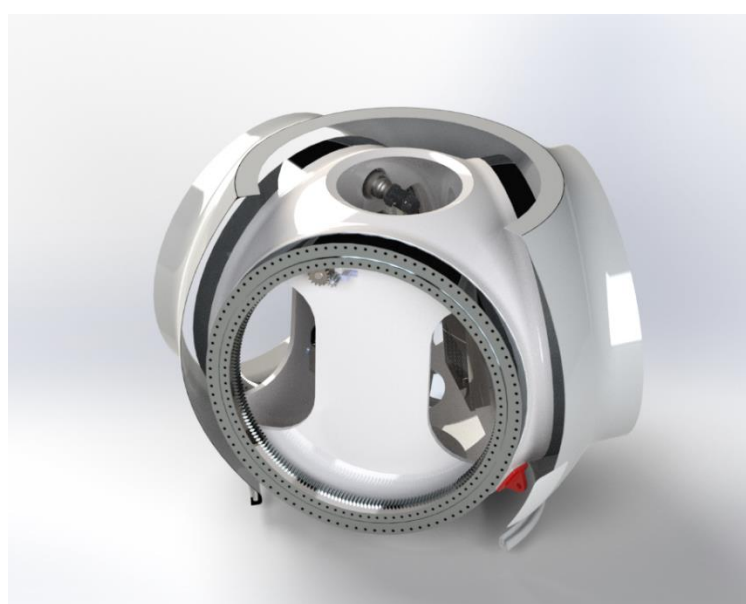


Figure:- 4. 39 : CAD model of Complete assembly of Rotor hub and pitch system

5. Maintenance strategies

Maintaining the rotor hub and pitch system of a wind turbine is vital for ensuring efficient, safe, and reliable operation. These key components play a crucial role in energy generation and control, and their malfunction can result in decreased performance, operational downtime, or severe damage. Outlined below is a component-specific overview of maintenance requirements:

Pitch Bearing

Inspection Content	Semi-Annual Maintenance	Annual Maintenance
Visual inspection of pitch bearing	✓	✓
Pitch bearing gear wear measurement	✓	✓
Gear ring and drive gear lubrication	✓	✓
Pitch bearing lubrication system inspection and grease filling	✓	✓
Torque maintenance of bearing-hub bolts	Visual Inspection	✓

Table: 5. 1: Maintenance startagies for Pitch bearing, Source [42]

Pitch System

Inspection Content	Semi-Annual Maintenance	Annual Maintenance
Blade zero-degree inspection	✓	✓
Torque maintenance for pitch control cabinet support bolts	Visual Inspection	✓
Pitch gear box oil level check	✓	✓
Pitch gearbox oil Change (Every 5 Years)	-	-
Pitch gearbox bearing lubrication (every 5 years)	-	-
Check the marking lines of pitch motor fixing bolts	Visual Inspection	✓
Torque maintenance of gearbox and hub connecting bolts	Visual Inspection	✓
Battery voltage inspection	✓	✓
Sensors Inspection	✓	✓

Table: 5. 2: Maintenance startagies for Pitch system [42]

Hub and Spinner

Inspection Content	Semi-Annual Maintenance	Annual Maintenance
Spinner inspection	✓	✓
Visual inspection of spinner bracket connecting bolts	✓	✓
Hub cleaning	✓	✓
Torque maintenance of foot pedal and hub connecting bolts	Visual Inspection	✓
Torque Maintenance of Hub and Shaft connection bolts	Visual Inspection	✓

Table: 5. 3: Maintennace startagies for hub and spinner [42]

6. Weight and cost

While one of our priorities in the design process was ensuring the availability of the designed components in the Indian market, we have calculated the weight and price of the components below

Item	Qty	Weight per unit (kg)	Weight (kg)
Rotor Hub	1	36,705.5	36,705.5
Blade bearing	3	7,890	23,670
Pitch motor and brake	3	384	1,152
Pitch Gearbox	3	345	1,035
Pinion	3	54.77	164.31
Spinner	1	1,980	1,980
Lubrication pinion	3	1	3
Lubrication pump	3	20	60
Bolt M39 (bearing-blade & shaft-hub)	536	2.36	1,264.96
Bolt M42 (bearing-hub)	435	2.76	1200.6
Bolt M20 (pitch motor- hub)	36	0.422	15.19
Total weight			67,250.56 kg

Table: 6. 1:Weight of the components

In addition, below you can find our estimation for component's prices:

Item	Qty	Cost per unit (€)	Cost (€)
Rotor Hub	1	155,556	155,556
Spinner	1		
Pitch drive	3	6,333	19,000
Blade bearing	3	40,000	120,000
Lubrication equipment	3	2,200	6,600
Fastening components and cable	--	3,200	3,200
Electrical components	3	36,000	108,000
Total costs			412,356 €

Table: 6. 2: Cost of the components

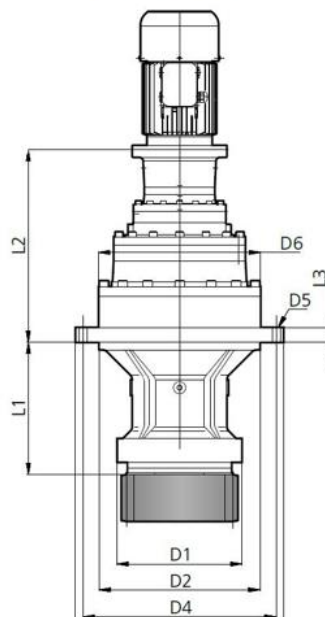
7. Specifications of Components

Pitch System

Pitch System	
Pitch drive type	Electrical pitch drive
	Internal drive
Gear box	3 stage planetary
Motor type	Synchronous AC reluctance(18.5 kW)
Max. pitch rate	6° per second
Max. pitch torque	612 kNm
Back-up system	Battery
Total gear ratio	2305
Weight of Pitch drive	0.4 T/Axis
Pinion Module	16
Number of teeth on pinion	16
Width of Pinion	162.5 mm

Table: 7. 1: Specification of Pitch system components

Inline version
Planetary gearbox



Type	Version	D1	D2	D3	D4	D5	D6	L1	L2	L3
711T	N	300	425	500	460	Ø 22 n°12	428	350	520	40

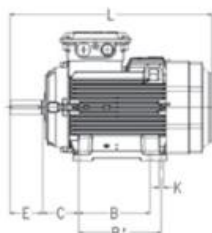
Figure: 7. 1 Bonfiglioli 711 TW gearbox dimensions [43]

Motor

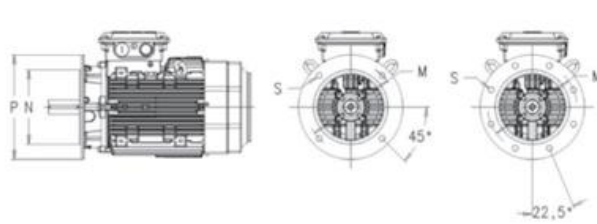
Motor	
Motor Type	Synchronous AC reluctance
Designation	M3BL200MLA4
IE class	IE5
Motor Efficiency	95.20%
Maximum Speed	4500 rpm
Current	39.9 A
Torque	177 Nm
Weight	304 Kg

Table: 7. 2: Specification of Pitch system components

Foot-mounted motor IM 1001, IM B3



Flange-mounted motor IM 3001, IM B5



Main dimensions for IE5 SynRM motors (C-generation)

Motor size	Speed r/min	IM1001, IMB3 and IM3001, IM1001, IMB3 IMB5										IM B5 (IM3001)					IM B14 (IM 3601), IM 3602						
		D	GA	F	E	L max	A	B	B1	C	H	HD max	K	M	N	P	S	T	M	N	P	S	T
200 MLA-F	3000-1000	55	59	16	110	821	318	267	305	133	200	528	18.5	350	300	400	19	5	350	300	400	19	5

Figure: 7. 2: ABB SynRM, frame size 200, dimensions [22]

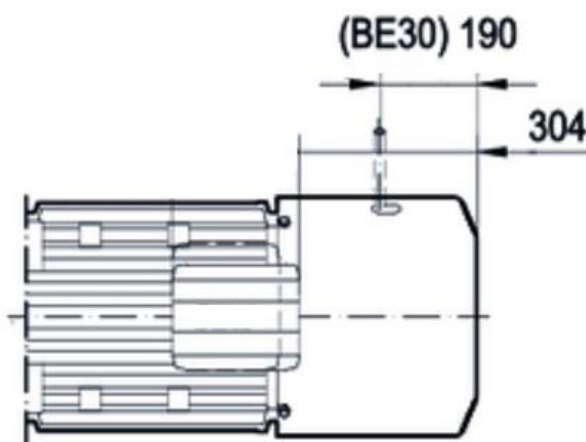


Figure: 7. 3: SEW-EURODRIVE, magnetic brake BE30 Dimensions [23]

Lubrication Pinion

Lubrication Pinion	
Material	Polyurethane (PU)
Number of teeth	8
Module	16
Maximum admissible volume flow	2 l/m ²
Maximum speed	80 rpm
Operating temperature	-30 to 70

Table: 7. 3: Specification of Pitch system components

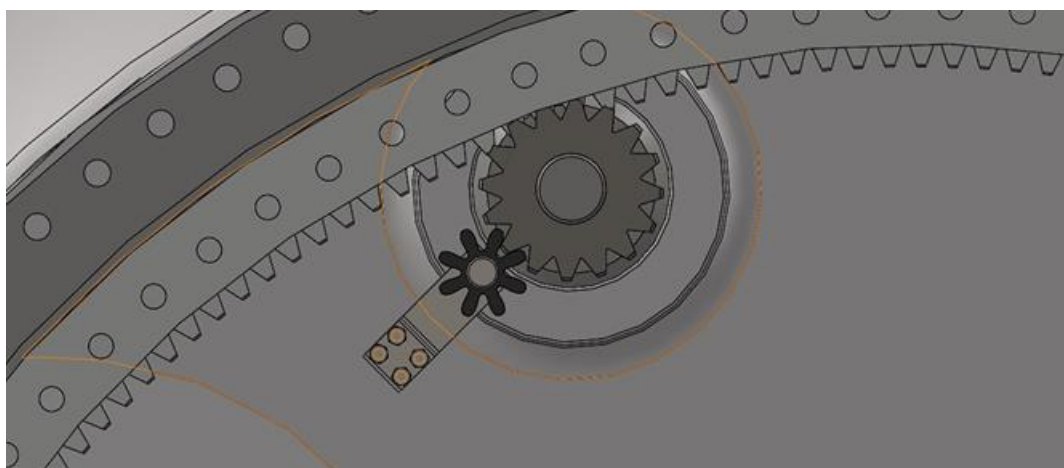


Figure: 7. 4: Lubrication pinion assembly of Optimus shakti

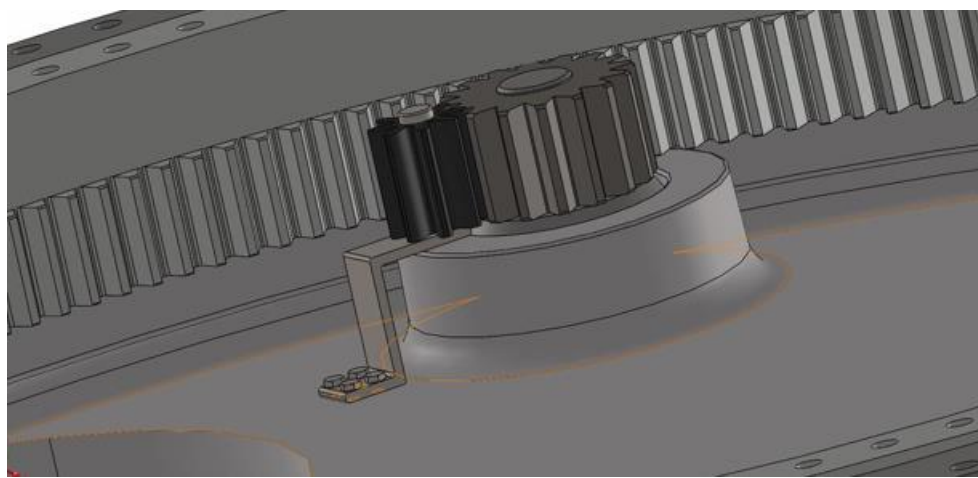


Figure: 7. 5: Lubrication pinion assembly of Optimus shakti

8. Environmental Life-Cycle Assessment

As a renewable energy source, wind power has assumed a significant role in the global energy transition. Nevertheless, the environmental impact of wind power is not entirely negligible. The manufacturing of wind turbines, which involves energy-intensive processes, is a notable contributor to carbon dioxide (CO₂) emissions. These emissions primarily arise from two key sources: the materials used in turbine components and the energy consumed during production.

Although operational wind turbines are ecologically beneficial due to their lack of direct emissions and minimal energy requirements, research findings indicate that the majority of environmental impacts are associated with the manufacturing and installation phases. As with all energy generation systems, the conversion of natural resources into usable energy carries inherent environmental consequences.

A critical study by Haapala (2014) employed the Life Cycle Assessment (LCA) method, facilitated by the SimaPro 7.3 software tool, to assess the environmental impacts of two 2.0 MW onshore wind turbine designs. This research highlighted key turbine components, including the rotor assembly, nacelle, and tower, which contribute significantly to environmental impacts due to their material composition and energy-intensive manufacturing processes. The study also underscored the significance of transportation emissions, calculated in terms of ton-kilometers (tkm), and the pivotal role of end-of-life recycling in mitigating environmental impacts. Recycling rates of up to 90% for materials like steel, copper, aluminum, and cast iron led to a substantial reduction in lifecycle emissions, while non-recyclable materials, such as concrete, were disposed of in landfills.

This chapter builds upon the methodology and insights from Haapala's research to estimate the CO₂ emissions and environmental impacts associated with specific wind turbine components. The focus is on the material composition, manufacturing processes, transportation logistics, and end-of-life scenarios.

Material Emission Calculation

The initial step in evaluating the carbon dioxide (CO₂) emissions of wind turbine components is to calculate material-specific emissions. The materials utilized in these components, including EN-GJS-400-18 cast iron, 42CrMo4 alloy steel, and glass fiber, possess distinct emission factors, which are expressed in kilograms of CO₂ per kilogram of material (kg CO₂/kg). By multiplying the weight of each material by its corresponding emission factor, the manufacturing emissions for each component can be determined. For instance, EN-GJS-400-18 contributes 0.70 kg CO₂ per kilogram, making it a significant contributor to overall emissions due to its extensive use in heavy parts like the rotor hub.

Transportation Emissions

Transportation of the components contributes additional CO₂ emissions, particularly for projects requiring long-distance shipping. Assuming that all parts are shipped from China to

India, emissions are calculated based on the distance traveled and the weight of the components. The journey involves sea freight over approximately 6,000 kilometers, followed by road transport for 500 kilometers to the installation site. Emission factors of 0.015 kg CO₂/ton-km for sea freight and 0.1 kg CO₂/ton-km for road transport are applied. A 50% load factor is assumed to account for return trips of empty vehicles.

End-of-Life Impact

The final stage of a product's lifecycle involves the recycling or disposal of the materials utilized in its components. Recycling rates of 90% for metals such as steel, cast iron, and aluminum can reduce overall environmental impacts by offsetting the emissions associated with the production of new materials. However, glass fiber is not recyclable and is typically sent to landfills, which can negatively impact the environmental profile. Properly managing the end-of-life treatment of materials can significantly mitigate lifecycle emissions and enhance sustainability.

Results

The total CO₂ emissions for each component, combining material, transportation, and end-of-life impacts, are summarized in the table below:

Component	Material Emissions (kg CO ₂)	Transportation Emissions (kg CO ₂)	Total Emissions (kg CO ₂)
Rotor Hub	25,712.58	5,142.52	30,855.10
Inner Ring Bearing	21,970.09	1,809.30	23,779.39
Outer Ring Bearing	19,577.27	1,612.25	21,189.51
Spinner	10,458.56	976.13	11,434.69
Lubrication (Oil & Grease)	150.00	18.75	168.75

Table: 8. 1 :-Co2 Emision from the Components lifecycle

9. Teamwork

The design and development of the rotor hub and pitch systems for the 5MW onshore wind turbine, Optimus Shakti, was a collaborative endeavor undertaken by a team of three members. Our team adopted a well-structured approach, dividing the project into specific tasks that leveraged each member's strengths and areas of expertise. Effective communication channels were established to ensure consistent updates and seamless coordination. Additionally, we conducted weekly meetings within the team and with the project manager and supervisor to review progress, address challenges, and align objectives, fostering a cohesive and supportive working environment.

This project offered a valuable opportunity to contribute to a large-scale design, allowing us to translate theoretical knowledge into practical solutions for complex engineering challenges.

Harmonizing the design of the rotor hub and pitch system required numerous iterations and thorough cross-validation, making the process time-intensive. Additionally, restricted access to technical references at times hindered progress. Nevertheless, our team exhibited resilience and strong problem-solving skills, devising innovative solutions and effectively managing time to overcome these challenges.

Ultimately, we successfully developed a robust and efficient rotor hub capable of withstanding operational loads, along with an optimized pitch system that effectively balances aerodynamic performance and load mitigation.

This project not only enhanced our technical skills but also highlighted the importance of teamwork, illustrating how collaboration and determination can drive successful outcomes.

Given table shows distribution of work among the team members

Section	Task Name	Report Writer	Contributors (Design and Calculations)
	Introduction	Islam M.	--
	Relevant standards and guidelines	Rahul P.	--
	Loads	Rahul P.	--
	Rotor Hub	Islam M., Rahul P.	Mostafa M., Rahul P
4.1.1	Shapes of the Hub	Islam M., Rahul P.	
4.1.2	Material of the Hub	Rahul P., Mostafa M.	
4.1.3	CAD design and dimension	Rahul P., Mostafa M.	Rahul P., Mostafa M.
4.2.1	Classification of Pitch System	Rahul P.	Mostafa M., Rahul P
4.2.2	Comparison between different concepts	Rahul P.	
4.2.3	Electric pitch System	Mostafa M.	Mostafa M.
4.2.3.3	Back-up supply System	Islam M.	Islam M.

4.3	Blade bearing	Rahul P.	Mostafa M., Rahul P
4.3.1	Types of bearing		
4.3.2	Blade attachment		
4.3.3	Bearing design	Mostafa M., Rahul P	Mostafa M., Rahul P
4.3.4	Safety factor for bearing teeth	Rahul P.	Rahul P.
4.3.5	CAD Model of Bearing	Mostafa M. Rahul P	Mostafa M. Rahul P
4.4	Bolted Joint Connection between hub and shaft	Rahul P.	Rahul P.
4.5	Bolted joint between hub and bearing	Rahul P.	
4.6	Lubrication system	Islam M.	Islam M.
4.7	Spinner	Mostafa M., Rahul P	Mostafa M., Rahul P
5.	Maintenance strategies	Mostafa M., Rahul P	
6.	Weight and Cost	Islam M., Mostafa M.	Islam M., Mostafa M.
7.	Specification of Components	Mostafa M.	--
8.	Environmental Life-Cycle Assessment	Islam M.	--
9.	Teamwork	Islam M., Rahul P., Mostafa M.	--
10.	Lesson learned	Mostafa M., Rahul P., Islam M.	--
11.	Report formatting	Mostafa M. Rahul P	

Table: 9. 1: Work Distribution in Team

10. Lesson Learned

The Optimus Shakti project, focused on designing the hub and pitch systems for a 5 MW onshore wind turbine, provided invaluable experiences and insights. Below are the key lessons we learned during this project.

We worked extensively to meet weekly presentation deadlines, which required disciplined planning and efficient time management.

Regular presentations throughout the project significantly enhanced our presentation skills. We became more confident in delivering technical content effectively and addressing questions from our peers and supervisors.

Collaboration within the team and with supervisors improved our communication skills, teaching us how to articulate ideas clearly and maintain effective teamwork.

We gained detailed technical knowledge of the design concepts for hub and pitch system components, including their functionality, materials, and structural considerations.

The project allowed us to work extensively with tools like SolidWorks for mechanical design and MATLAB for analysis, improving our proficiency in these industry-relevant software applications.

Planning the project to achieve deadlines taught us how to break down a complex task into manageable phases, allocate resources effectively, and adapt plans as needed to overcome challenges.

11. Conclusion and Outlook

The Optimus Shakti project marks a major advancement in creating a durable and efficient 5 MW onshore wind turbine designed specifically to withstand India's demanding climatic conditions. Our team effectively developed key components such as the rotor hub, a three-row roller pitch bearing, and an electric pitch system, ensuring exceptional reliability and performance.

By integrating a state-of-the-art lubrication system for the pitch bearing and its teeth, we have significantly improved durability and minimized maintenance requirements, which are essential for operation in harsh environments. Furthermore, the spinner was carefully engineered to enhance aerodynamic efficiency while enduring the extreme weather conditions prevalent in India.

We are confident that the Optimus Shakti wind turbine is well-suited to meet the specific requirements of the country's diverse and challenging weather conditions.

Outlook

The Hub and Pitch Actuator team in wind turbine design projects typically begins its work after the Load team provides the overall design dimensions and initial data. However, for this project, the limited timeframe meant that the Load team started from scratch simultaneously with us. This presented a significant challenge, as key inputs such as dynamic forces and initial dimensions were not readily available.

To overcome this, we adopted two primary strategies:

Utilization of Market Data: We relied on data from existing wind turbines of similar capacity available in the market.

Flexible Computational Framework: We organized the computational process in MATLAB to allow for easy updates and modifications. This approach ensured that once the Load team finalized their input, we could seamlessly adjust the calculations and obtain more precise results.

Despite these efforts, certain tasks faced inherent limitations due to the lack of initial data:

FEM Analysis of the Hub: Accurate modeling of dynamic forces and stresses over time was not achievable at the desired level of precision without comprehensive input data.

Actuator Design: Dynamic control behavior and torque-power characteristics under varying conditions were essential for selecting a suitable market product. Limited data constrained this analysis.

Blade Bearing Analysis: While initial analytical calculations were completed, transitioning to FEM-based analysis would provide more reliable results for higher accuracy.

Future Steps

Collaboration with the Load team to incorporate dynamic forces and other missing inputs will allow more precise simulations and analyses.

Finalizing FEM analysis for the hub and blade bearings to ensure reliability under operational conditions.

Refining actuator selection by analyzing its performance based on updated torque and speed requirements.

Expanding the MATLAB code to handle more complex scenarios, such as transient load conditions, for improved adaptability.

References

- [1] W. o. M. o. n. a. r. e. India, „Ministry of new and renewable energy: India,” November 2024. [Online]. Available: <https://mnre.gov.in/wind-overview/>.
- [2] DNV-ST-0361, Machinery for wind turbines, DNV GL, September, 2016.
- [3] GL, „Guidelines for certification of the wind turbines,” GL, 2010.
- [4] Mr.christian Bulligk, *Three Rows roller bearing Dimensioning of the Raceway system & Loads*, Flensburg, 2024.
- [5] G. Erich Hau Dipl.–Ing Munich, Wind Turbines Fundamentals, Technologies, Application, Economics, Munich, 2012.
- [6] R. Gasch und J. Twele, Wind Power Plants: Fundamentals, Design, Construction and Operation, Berlin/ Heidelberg: Springer, 2012.
- [7] G. H. Mehdi Shirania, „A review on fatigue design of heavy section EN-GJS-400-18-LT ductile iron wind turbine castings,” *Energy Equipment and Systems*, Bd. 1, p. 2, 2014.
- [8] „Modulus Metal,” 06 11 2022. [Online]. Available: <https://www.modulusmetal.com/2022/11/06/en-gjs-400-18-mechanical-properties/>. [Zugriff am 03 01 2025].
- [9] P.-i. H. W. Proff. Peter Quell, „Rotor Hub and flanges,” in *Machinery Components* , 2024.
- [10] „IFM Electric pitch drive,” IFM, 2024. [Online]. Available: <https://www.ifm.com/de/en/shared/machine/energy/wind-energy/electric-pitch-drive>. [Zugriff am 03 01 2025].
- [11] MNRE, „Revised List of Models & Manufacturers (RLMM) of,” Ministry of New and Renewable Energy (MNRE), 2023. [Online]. Available: <https://cdnbbsr.s3waas.gov.in/s3716e1b8c6cd17b771da77391355749f3/uploads/2023/10/202310182121995669.pdf>. [Zugriff am 04 01 2025].
- [12] I. D. SARAC V., „“Synchronous Motor of Permanent Magnet compared to Asynchronous Induction Motor”,“ *Electrotehnica, Electronica, Automatica (EEA)*, , Bde. %1 von %2, vol. 65, Nr. ISSN 1582-5175, pp. no. 4, pp. 51-58,, 2017.
- [13] U. o. Tennessee. [Online]. Available: https://web.eecs.utk.edu/~kaisun/Backup/ECE325_Fall2016/ECE325_6-InductionMotors_4.pdf. [Zugriff am 01 01 2025].
- [14] &. A. P. &. A.-A. I. &. A. Enesiasizehiyahaya, „Analysis of Power flow and Torque of Asynchronous Induction Motor Equivalent circuits. 3.,“ 2013.

- [15] B. M. S. B. I. M. A.Y. Achour, „Passivity-based current controller design for a permanent-magnet synchronous motor,“ ,*ISA Transactions*, Bd. Volume 48, Nr. Issue 3,2009, <https://doi.org/10.1016/j.isatra.2009.04.004..>
- [16] M. Ç. Yıldırım ÖZÜPAK, „DESIGN OF THE PERMANENT MAGNET SYNCHRONOUS MOTOR USED IN ELECTRIC VEHICLES WITH THE HELP OF THE PARTICLE SWARM ALGORITHM AND ANSYS-MAXWELL,“ 21 01 2025. [Online]. Available: <https://dergipark.org.tr/en/download/article-file/3212091>.
- [17] H. R. A. K. A. V. T. A. E. B. A. &. L. D. V.] Heidari, „A Review of Synchronous Reluctance Motor-Drive Advancements. Sustainability, 13(2), 729,“ Bd. 13(2), Nr. <https://doi.org/10.3390/su13020729>, 2021.
- [18] M. C. Vladan Vujičić, „Characteristics of Switched Reluctance Generator operating with Derishzadeh converter,“ in *IcETRAN* , Zlatibor, Serbia, 2016.
- [19] “Direct Current Motors.” CEDS Duradrive, CEDS Duradrive, [Online]. Available: [www.ceds-duradrive.de/en/technologien/direct-current-motors/..](http://www.ceds-duradrive.de/en/technologien/direct-current-motors/) [Zugriff am 26 11 2024].
- [20] K. B. P. F. Jan Wenske, Wind Turbine System Design. Volume 1: Nacelles, drivetrains and verification, IET - The Institution of Engineering and Technology, December 2022.
- [21] L.-C. A. (n.d.), „Slewing bearings;“ Product catalogue. Liebherr., [Online]. Available: https://www-assets.liebherr.com/media/bu-media/lhbucot/documents/cot_grosswaelzlager/sticky_notes/liebherr-slewing-bearings-product-catalogue-en-metric-web.pdf. [Zugriff am 08 12 2024].
- [22] ABB., Low voltage IE5 Synchronous reluctance motors. ABB., 2023. [Online]. Available: https://library.e.abb.com/public/d9f6455b71c7496eb1368e3e5937358d/9AKK107743_IEC%20LV%20Synchronous%20reluctance%20motors_09-2023_lowres.pdf. [Zugriff am 24 12 2024].
- [23] SEW-EURODRIVE, „BRAKE,“ [Online]. Available: https://download.sew-eurodrive.com/download/pdf/22134204_G07.pdf. [Zugriff am 20 01 2025].
- [24] Kurt.Energy, „eric verhulst 2024 Wind turbine pitch control and emergency shutdown,“ <https://kurt.energy/wind-turbine-pitch-control-and-emergency-shutdown/>, (accessed 28 Dec 2024).
- [25] J. W. J. Q. a. Q. H. Bixiao G, „The Lithium-ion Battery Standby Power of Wind Turbine Pitch System Energy Procedia,“ p. 105 3539–44, 2017.
- [26] Battery, „Delta Batteries,“ Delta, 2024. [Online]. Available: <https://www.delta-emea.com/en-GB/products/Lithium-Ion-Battery/TBM48V050-LF1>.

- [27] Delta, „Specification of the batteries,“ Delta Batteries, 2024. [Online]. Available: https://filecenter.deltaww.com/Products/download/09/0912/Catalogue/Fact-sheet_TPS-Battery_IP65-48V50Ah-LIB_en_230815.pdf.
- [28] X.-U. S. Tripower, „SMA,“ STP 251JS-50, 2024. [Online]. Available: chrome-extension://efaidnbmnnibpcajpcglclefindmkaj/https://files.sma.de/assets/279316.pdf.
- [29] K. a. B. A. &. B. E. &. G. Behnke, Pitch systems concepts ans Design, 2022.
- [30] „thyssenkrupp-rotheerde,“ thyssenkrupp-rotheerde, 08 11 2024. [Online]. Available: <https://www.thyssenkrupp-rotheerde.com/en/industries/renewable-energy/wind-energy/pitch-bearing>. [Zugriff am 03 01 2025].
- [31] „IMO,“ IMO-Slew drives and Slewing ring , 2016. [Online]. Available: https://www.youtube.com/watch?v=eVXnD0_L0c4. [Zugriff am 03 01 2025].
- [32] M. O. M. Y. G. a. J. K. Stammler, „Wind Turbine Design Guideline DG03: Yaw and Pitch Bearings,“ National Renewable Energy Laboratory (NREL), Bd. 2, 2024.
- [33] „SKF,“ SKF bearing, 2024. [Online]. Available: <https://www.skf.com/group/products/rolling-bearings/ball-bearings/angular-contact-ball-bearings/double-row-angular-contact-ball-bearings>. [Zugriff am 03 01 2025].
- [34] „Senvion Products,“ 2024. [Online]. Available: <https://www.senvion.in/products/4-2m160/>. [Zugriff am 03 01 2025].
- [35] D. e. a. Muhs, Roloff/Matek Maschienenelemente, Normung Berechnung Gestaltung, Auflage; Wiesbaden Friedr. Vieweg & Sohn Verlag/GWV Fachverlag GmbH, 2005.
- [36] S. Krishnan, „A Comparative Review of the Lubrication of Bearings in Wind Turbines and Spacecraft to Address Wind Turbine Bearing Failures,“ In *Tribol. Ind.* 45 (1) DOI: 10.24874/ti.1452.02.23.05., Bd. 01, p. pp. 257–271., 2023.
- [37] SKF, „SKF bearing maintenance handbook,“ SKF bearings , 2011. [Online]. Available: https://cdn.skfmediahub.skf.com/api/public/0901d1968013be94/pdf_preview_medium/0901d1968013be94_pdf_preview_medium.pdf. [Zugriff am 06 12 2024].
- [38] 61400-1, „ Wind Energy Generation System,“ IEC Standards, 2019.
- [39] F. L. Germany, „FUCHS Lubricants Germany,“ 01 2025. [Online]. Available: <https://www.fuchs.com/de/de/produkt/product/148104-GLEITMO-585-K-PLUS/>.
- [40] „SKF,“ SKF-LP02-Lubrication pinion, 2024. [Online]. Available: https://cdn.skfmediahub.skf.com/api/public/0901d196806c2ca9/pdf_preview_medium/0901d196806c2ca9_pdf_preview_medium.pdf.

- [41] Kaufmann, „Are Wind turbines rotor blades sustainable,” 2024. [Online]. Available: <https://www.dw.com/en/can-wind-turbine-rotor-blades-ever-be-sustainable/a-59834219>.
- [42] Envision, „Envision Wind Power,” 2025. [Online]. Available: <https://www.envision-group.com/en/windturbines.html>.
- [43] ". S. S. D. Y. & P. D. Bonfiglioli, Bonfiglioli, [Online]. Available: https://www.bonfiglioli.com/international/en/product/700-tw-series_slew-drives_yaw-pitch-drives. [Zugriff am 01 01 2025].
- [44] DNV/Risø, Guidelines, Copenhagen: DNV/Risø, 2002.
- [45] L. Krishnappa, „Fatigue Analysis of a Generic 7.5 MW,” TUM, p. 86, 2016.
- [46] L. Tartibu, „A simplified analysis of the vibration of variable length blade as might be used,” ResearchGate, p. 136, 2008.
- [47] W. 3. k. w. t. generator, „wind-turbine-models,” WindMaster, [Online]. Available: <https://en.wind-turbine-models.com/fotos?manufacturer=189&p=1>.
- [48] W. t. design, „Wikipedia,” 18 November 2024. [Online]. Available: https://en.wikipedia.org/wiki/Wind_turbine_design.

Annextures

A-Loads

B- Project Order

C- Rotor Hub Optimus Shakti

D- Pitch Bearing

E- Spinner of Optimus Shakti

F-Assembly of rotor hub and pitch system of Optimus Shakti

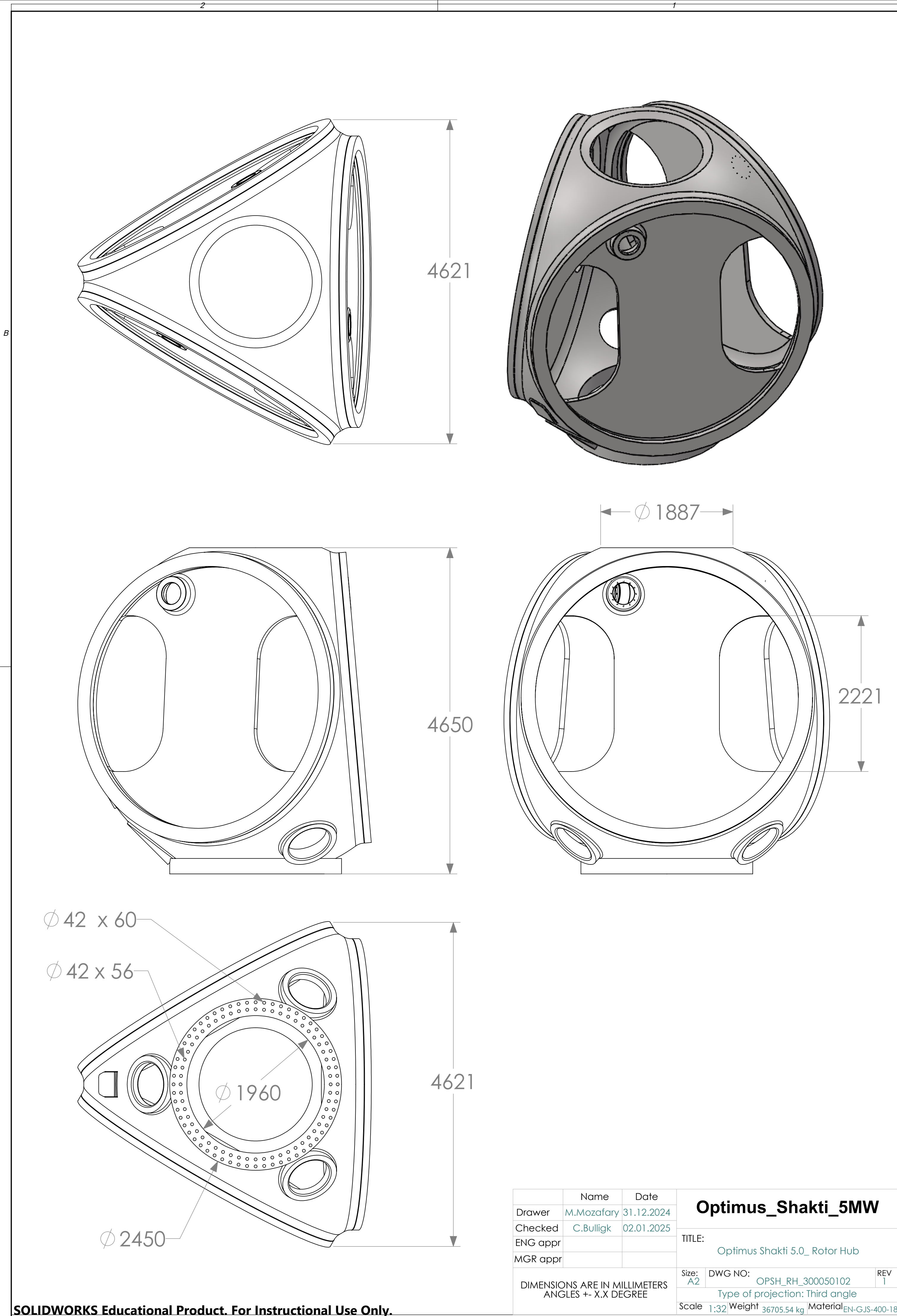
Fx	Fy	Fz	Fxy	Mx	My	Mz	Mxy
kN	kN	kN	kN	kNm	kNm	kNm	kNm
2311.686	2756	5770	3041	15520.71507	58162	34764	36646
Edgewise Bending Moment at Blade Root (MxS) versus Rotor Diameter							
Fx	Fy	Fz	Fxy	Mx	My	Mz	Mxy
kN	kN	kN	kN	kNm	kNm	kNm	kNm
1034.2868	779.428487	2737.190827	1908.5	23056.8	49553.14	619.6014125	31259.10259

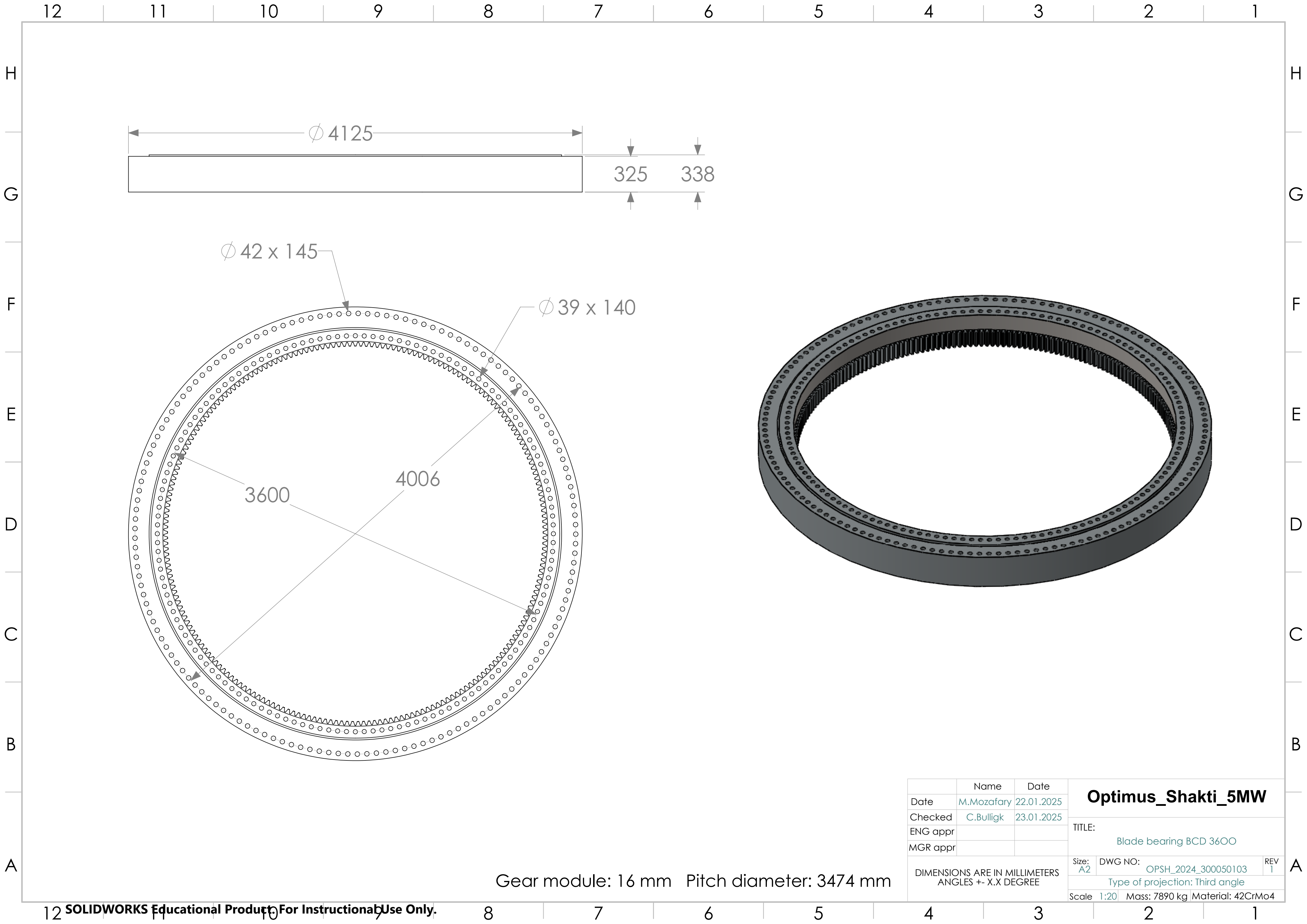
Rotor Thrust at Hub Center (FxN) versus Rotor Diameter							
Fx	Fy	Fz	Fxy	Mx	My	Mz	Mxy
kN	kN	kN	kN	kNm	kNm	kNm	kNm
3472.348	2119.336	6991.916	4117.76	29362.91	22268.72	28689.69	39788.58

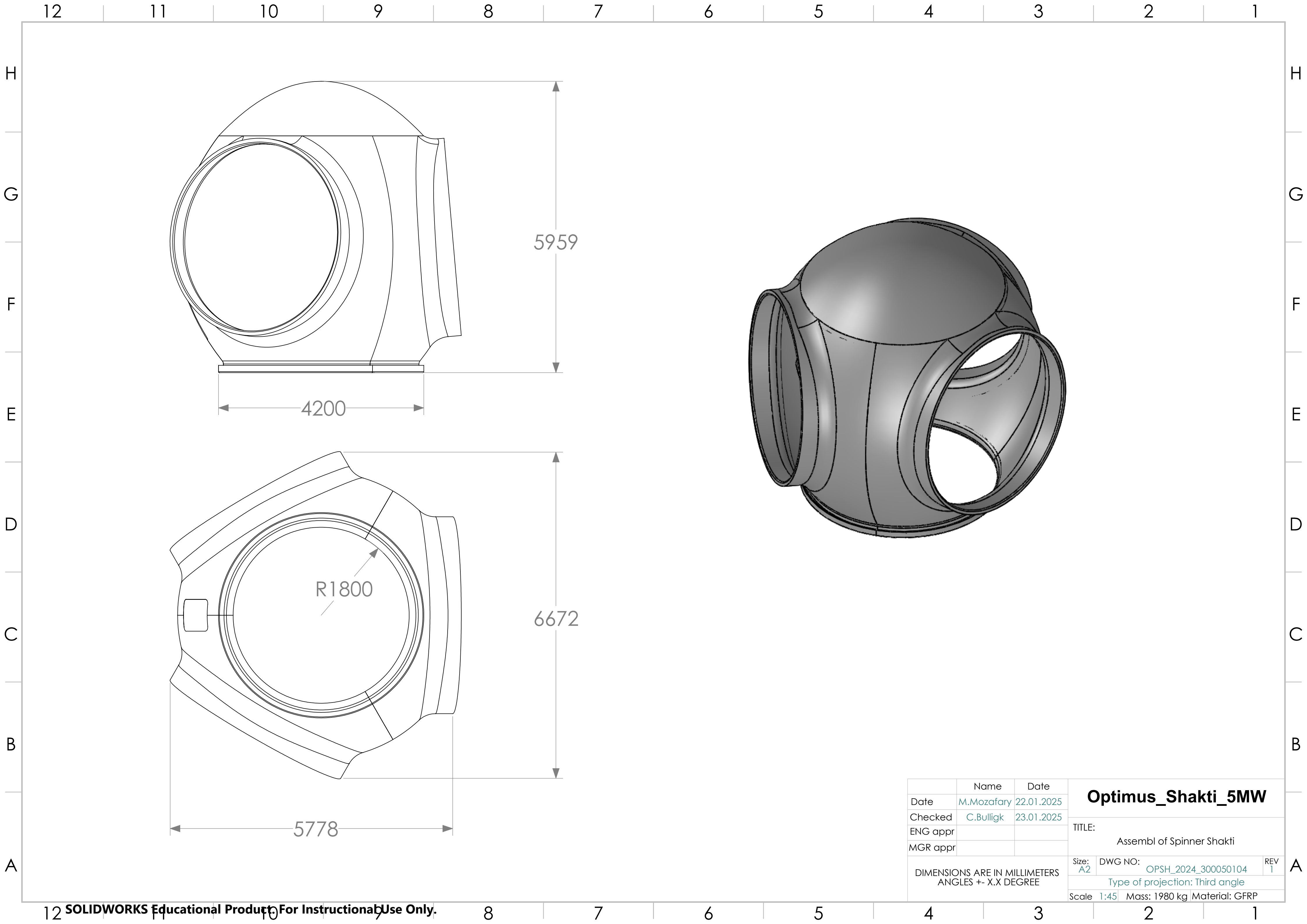
Flapwise Bending Moment at Blade Root (MyS) versus Rotor Diameter							
Fx	Fy	Fz	Fxy	Mx	My	Mz	Mxy
kN	kN	kN	kN	kNm	kNm	kNm	kNm
1034	779	2737	883	20665	51227	837	46697.9

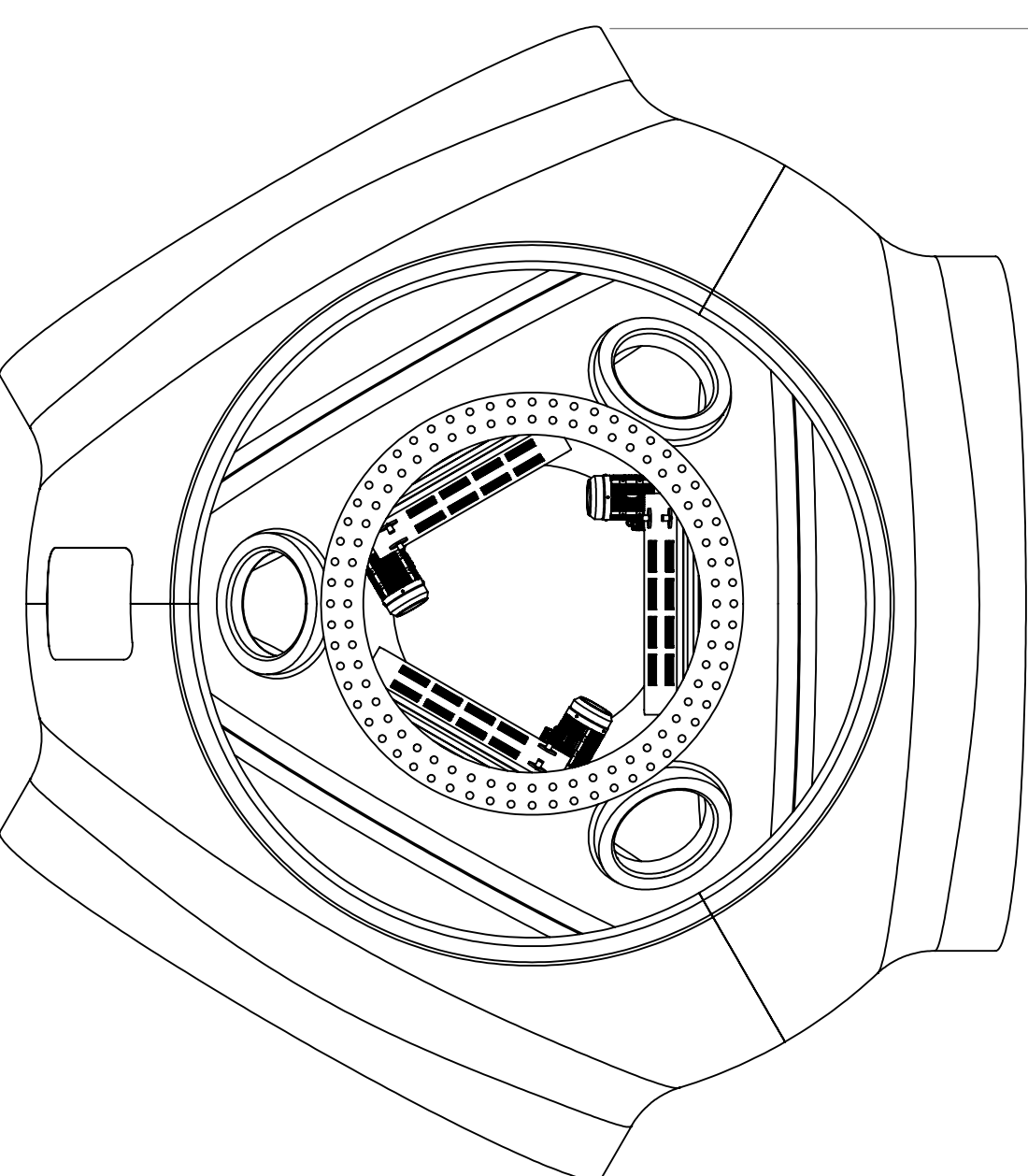
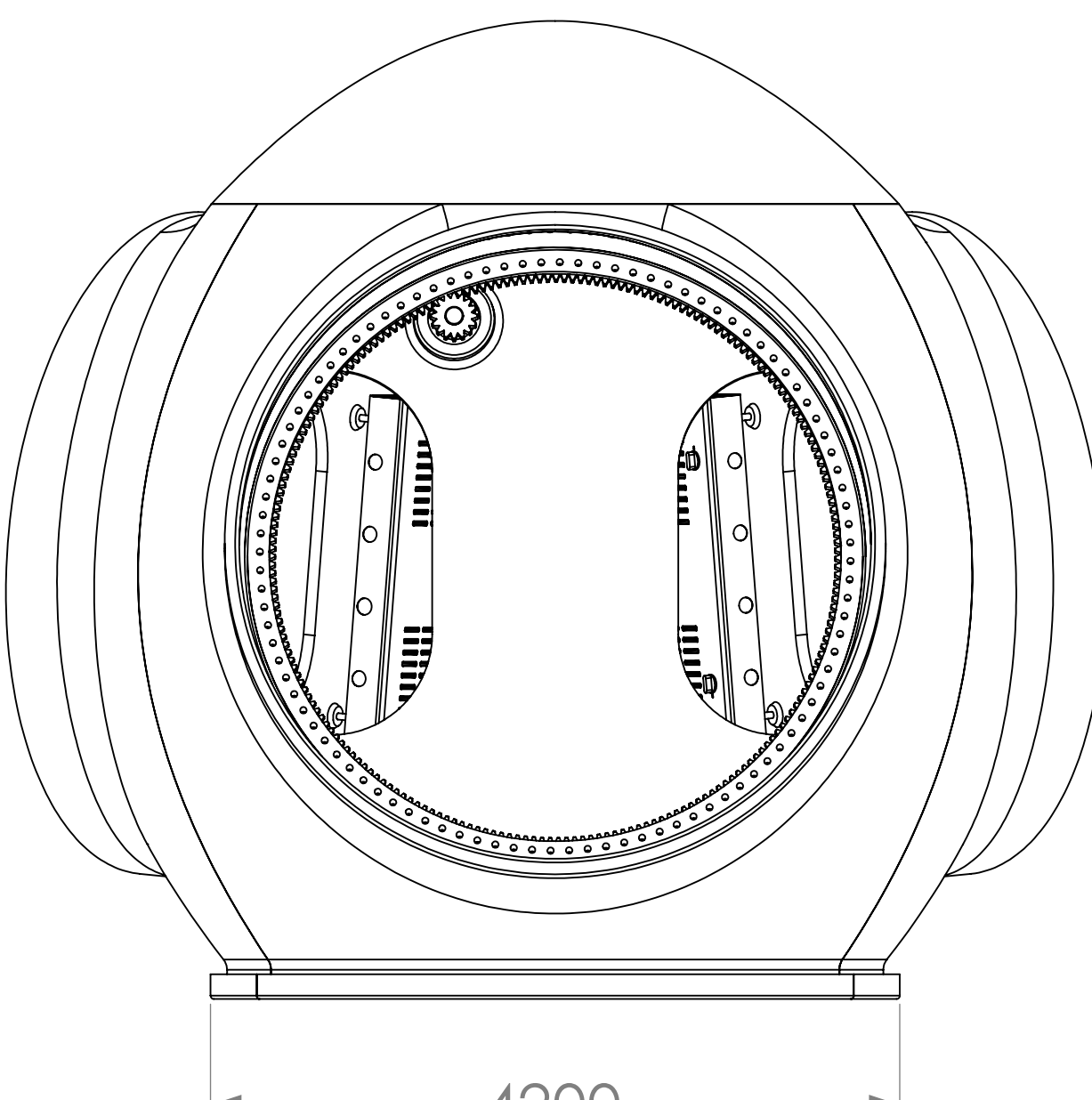
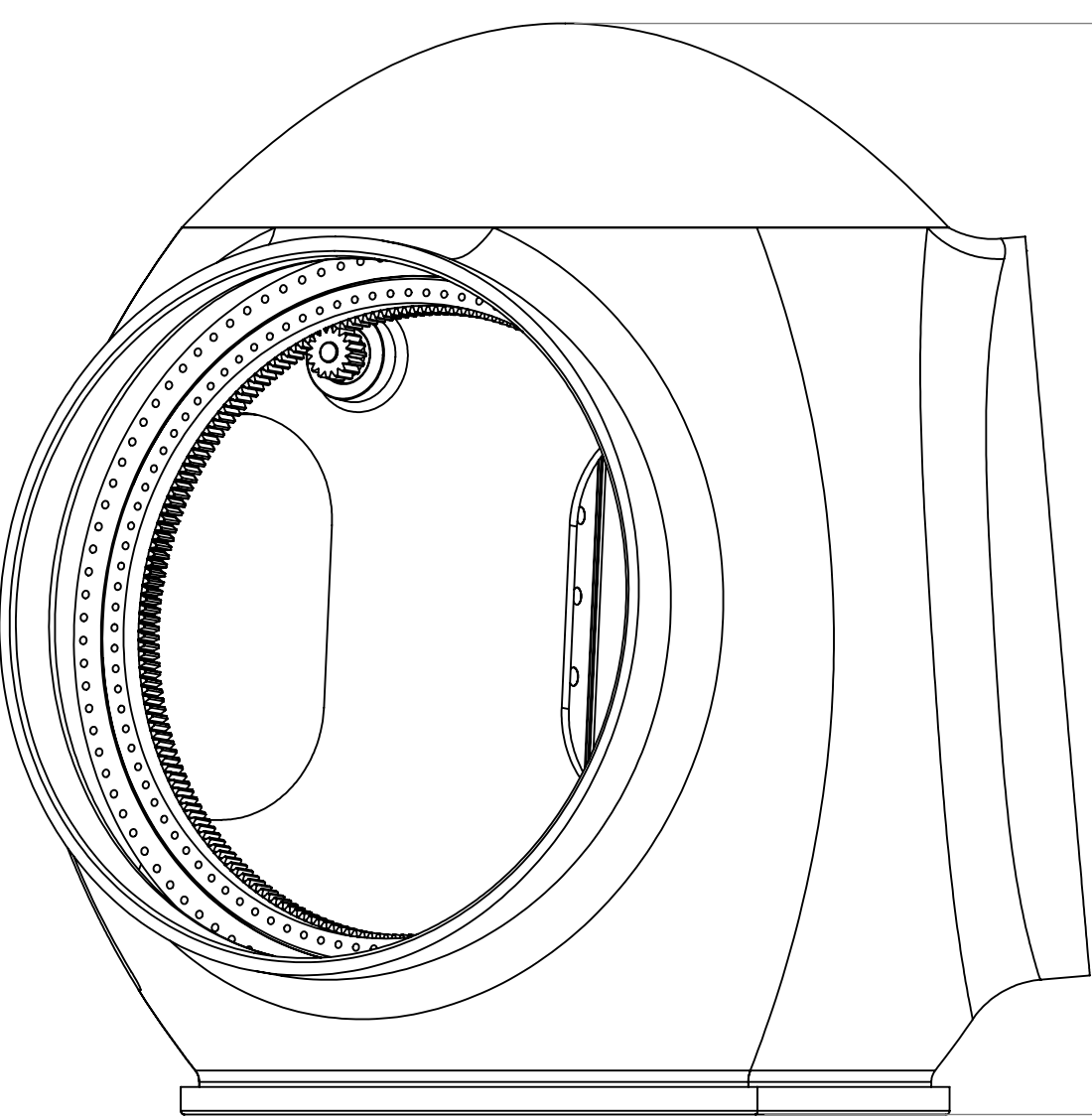
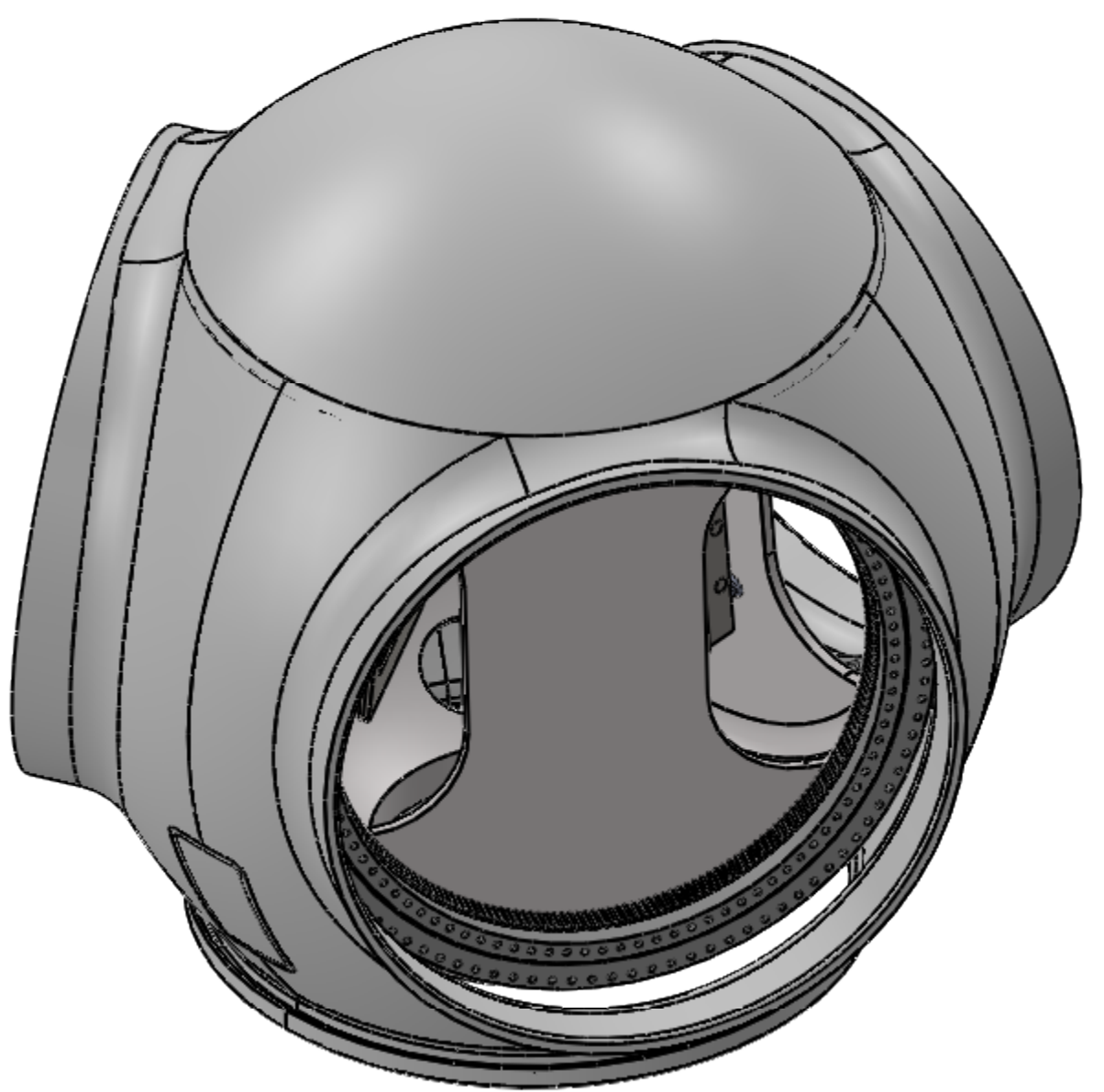
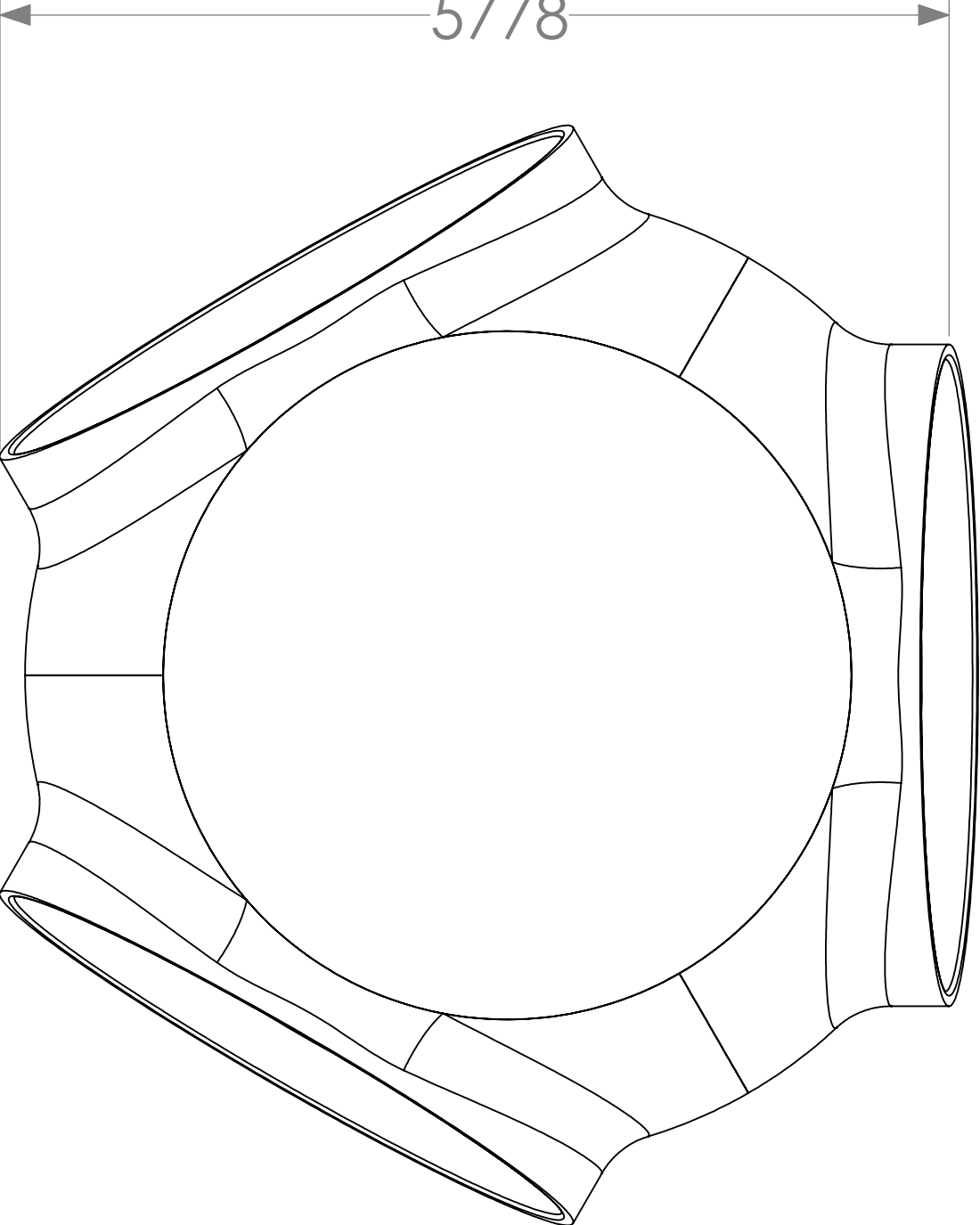
Rotor Torque at Hub Center (MxN/R) versus Rated Power							
Fx	Fy	Fz	Fxy	Mx	My	Mz	Mxy
kN	kN	kN	kN	kNm	kNm	kNm	kNm
1025.1	1110.1	1128.656	1268.66	5262	10261.39	9138.2	10552.96

Project Order						
Project Name:	Optimus Shakti	Project Number:	0.8			
Sub-Project	Rotor Hub & Pitch System	Project Manager	Mostafa Elbanna			
Customer:	Mr.Christian Bulligk	Deputy / SI:	Jannik Stegert			
Date:	15/10/2024	Team leader:	Rahul Patil			
Problem Description (Reason for the Project, Strategic Purposes):						
In this project, we want to design a 5 MW onshore wind turbine for the state of Karnataka, India, for low wind speed class area. At low wind speeds, the turbine experiences more irregular loading due to gusts or turbulence, putting additional stress on the pitch bearings and Pitch system. Frequent small adjustments in pitch angle (due to the lower and variable wind speeds) can cause fatigue loading on the bearings. This continuous load cycling can lead to premature bearing failure if not properly designed. In our sub-project, we will focus on designing the pitch system, pitch bearing, and hub for the targeted turbine, with the goal of creating an optimal design that can withstand the loads and efficiently transfer them to the machine bed.						
Project Objectives:						
To design of the Pitch System for our project						
To design of the Rotor Hub for our project						
To design the Pitch Bearing for the wind turbine						
To design Spinner for the Hub						
To provide the CAD model for the hub, spinner and pitch system						
Organisation (Committees, People, Responsibilities):						
Steering Committee:	Mr. Christian Bulligk, Mr.Mostafa Elbana, Mr.Jannik Stegert					
Project Team:	3rd semester 'Master Wind engineering' 2024/2025					
Team leaders:	Rahul Patil					
Sub-Project Team:	Mostafa Mozafary, Islam Mohamed, Rahul Patil					
Dates, Milestones						
Start of Project:	24th Sep 2024					
Team Organisation (People, Responsibilities)	24th Sep 2024					
Market research	1st Oct 2024					
Design of Pitch bearing	22nd Oct 2024					
Design of a Pitch System	29th Oct 2024					
Design of Rotor Hub	5th Nov 2024					
Design of Spinner	12th Dec 2024					
Project Report:	23th Dec 2024					
Final presentation / end of project:	28th Jan 2025					
Restrictions:						
Limited data available related pitch bearing dimension such as drawing or detailed specification, Timeline of the semester						
Risk Management (Which risks may occur, how to manage it?)						
Risk: Lack communication within the team	Measure: Arranging weekly meetings with supervisor and Team members					
Risk: Unmotivated team member	Measure: Encourage the team					
Risk: Lack of research and documentation	Measure: Ask supervisors and Suppliers for references					
Risk: Not able to get desired results within the timeline	Measure: Continuous motivation and hard work					
Reporting:						
Weekly presentation						
Weekly meeting with tutor						
Weekly meeting with group members						
Final report						
Final presentation						
Team leader:	Head of Project:					
Date: 29/10/2024	Date: 29/10/2024					
Signature: 	Signature:					









	Name	Date	Optimus_Shakti_5MW	
Drawer	M.Mozafary	31.12.2024		
Checked	C.Bulligk	02.01.2025		
ENG appr				
MGR appr				
DIMENSIONS ARE IN MILLIMETERS ANGLES + X.X DEGREE				
Size:	DWG NO:	OPSH_2024_300050101	REV	1
Type of projection:	Third angle			
Scale	1:41			